UC Irvine
UC Irvine Previously Published Works

Title

Quantitative Proteomics Analysis of VEGF-Responsive Endothelial Protein S-Nitrosylation Using Stable Isotope Labeling by Amino Acids in Cell Culture (SILAC) and LC-MS/MS1

Permalink

https://escholarship.org/uc/item/2dp005p1

Journal

Biology of Reproduction, 94(5)

ISSN

0006-3363

Authors

Zhang, Hong-Hai
Lechuga, Thomas J
Chen, Yuezhou
et al.

Publication Date

2016-05-01

DOI

10.1095/biolreprod.116.139337

Copyright Information

Peer reviewed

Quantitative Proteomics Analysis of VEGF-Responsive Endothelial Protein *S*-Nitrosylation Using Stable Isotope Labeling by Amino Acids in Cell Culture (SILAC) and LC-MS/MS[1]

Hong-Hai Zhang,[3] Thomas J. Lechuga,[3] Yuezhou Chen,[3] Yingying Yang,[4] Lan Huang,[4] and Dong-Bao Chen[2,3]

[3]*Department of Obstetrics and Gynecology, University of California, Irvine, California*
[4]*Department of Biophysics and Physiology, University of California, Irvine, California*

ABSTRACT

Adduction of a nitric oxide moiety (NO•) to cysteine(s), termed *S*-nitrosylation (SNO), is a novel mechanism for NO to regulate protein function directly. However, the endothelial SNO-protein network that is affected by endogenous and exogenous NO is obscure. This study was designed to develop a quantitative proteomics approach using stable isotope labeling by amino acids in cell culture for comparing vascular endothelial growth factor (VEGFA)- and NO donor-responsive endothelial *nitroso*-proteomes. Primary placental endothelial cells were labeled with "light" (L-$^{12}C_6$$^{14}N_4$-Arg and L-$^{12}C_6$$^{14}N_2$-Lys) or "heavy" (L-$^{13}C_6$$^{15}N_4$-Arg and L-$^{13}C_6$$^{15}N_2$-Lys) amino acids. The light cells were treated with an NO donor nitrosoglutathione (GSNO, 1 mM) or VEGFA (10 ng/ml) for 30 min, while the heavy cells received vehicle as control. Equal amounts of cellular proteins from the light (GSNO or VEGFA treated) and heavy cells were mixed for labeling SNO-proteins by the biotin switch technique and then trypsin digested. Biotinylated SNO-peptides were purified for identifying SNO-proteins by liquid chromatography-tandem mass spectrometry (LC-MS/MS). Ratios of light to heavy SNO-peptides were calculated for determining the changes of the VEGFA- and GSNO-responsive endothelial *nitroso*-proteomes. A total of 387 light/heavy pairs of SNO-peptides were identified, corresponding to 213 SNO-proteins that include 125 common and 27 VEGFA- and 61 GSNO-responsive SNO-proteins. The specific SNO-cysteine(s) in each SNO-protein were simultaneously identified. Pathway analysis revealed that SNO-proteins are involved in various endothelial functions, including proliferation, motility, metabolism, and protein synthesis. We collectively conclude that endogenous NO on VEGFA stimulation and exogenous NO from GSNO affect common and different SNO-protein networks, implicating SNO as a critical mechanism for VEGFA stimulation of angiogenesis.

endothelium, nitric oxide, SILAC, S-nitrosylation, VEGFA

INTRODUCTION

Nitric oxide (NO) is an essential signaling molecule that is critical for vascular health, participating in the regulation of numerous physiological and pathological processes [1]. Cogent evidence has accumulated to demonstrate a critical role of NO derived from endothelial NO synthase (NOS3) in mediating endothelial cell proliferation and migration during angiogenesis in response to vascular endothelial growth factor (VEGFA) [2–4]. However, the pathways after NO biosynthesis by which VEGFA regulates these cellular processes are largely unknown.

Generation of the second messenger cyclic guanosine monophosphate (cGMP) is the best-defined NO signaling [5]; however, many NO bioactivities are cGMP independent. NO can directly regulate protein function post-translationally [6]. Covalent adduction of an NO moiety (NO•) to reactive cysteines is called *S*-nitrosylation (SNO). SNO denotes the most crucial cGMP-independent NO signaling; its significance has been compared to homologous *O*-phosphorylation [7]. SNO is capable of regulating the proteome because reactive cysteine(s) are often present in the catalytic active sites of numerous enzymes [8]. Thus, SNO inevitably participates in many biological pathways, such as calcium signaling, apoptosis, redox signaling, and angiogenesis [6, 7, 9, 10]. Not surprisingly, malfunctions in this critical cellular process have been implicated as a causal factor in diseases such as diabetes, hypertension, preeclampsia, sepsis, cancer, and Alzheimer's [11–14]. Large-scale identification of SNO substrates will certainly advance the understanding of diverse biological phenomena, potentially leading to intervention in any number of disease paradigms.

Although SNO has been recognized as a crucial mechanism by which NO regulates protein function directly, the fragile S-NO bond could not be measured accurately until the biotin switch technique (BST) was invented [15]. In this method, SNO groups are selectively reduced by ascorbate and then labeled with biotin, allowing *nitroso*-proteins to be readily displayed, affinity purified, and identified. We have previously developed a comprehensive proteomics approach involving BST for labeling SNO-proteins, two-dimensional difference in gel electrophoresis (2D-DIGE) for protein separation, and matrix-assisted laser desorption/ionization time-of-flight (MALDI-TOF)/mass spectrometry (MS) for analyzing the *nitroso*-proteomes of estrogen-treated endothelial cells and normotensive versus preeclamptic human placentas [14, 16, 17]. This method is perhaps the most powerful one to date, capable of analyzing SNO-proteins at a large scale. However, it is also tedious, semiquantitative, and not truly unbiased and powerful enough for digging out the entire *nitroso*-proteome. Moreover, it cannot simultaneously identify the specific SNO

sites that are absolutely required for downstream functional analysis of SNO in each individual target protein.

An ideal large-scale identification approach for SNO-proteins should at least require specificity, high throughput, identification of proteins with specific SNO site(s), and unbiased quantitation. The powerful MS technology sequences thousands of peptides from complex mixtures without the need for protein separation, offering a simple and fast method for large-scale identification of proteins [18]. Among the many platforms of quantitative proteomics approaches, stable-isotope labeling by amino acids in cell culture (SILAC)/MS has emerged as a simple and powerful one [19]. SILAC, first described in 2002 [20], involves growing two populations of cells by metabolic labeling with stable isotopes: population A in a medium that contains the ''light'' (normal) essential amino acids (AA) and population B in a medium that contains the ''heavy'' ones. The heavy AA contains ^2H instead of H, ^{13}C instead of ^{12}C, or ^{15}N instead of ^{14}N. Incorporation of the heavy AA into a peptide leads to a known mass shift compared with the peptide that contains the light AA (e.g., 6 Da for $^{13}C_6$ vs. $^{12}C_6$) but to no other chemical changes. Then the cells are mixed (A/B = 1:1), and their proteomes are extracted for peptide sequencing by liquid chromatography-tandem mass spectrometry (LC-MS/MS). Each peptide appears as a pair in the mass spectra: one with lower mass contains the light AA from population A, and the other with higher mass contains the heavy AA from population B. Because the light and heavy AAs are chemically identical, except for their mass difference, the ratio of the peak intensities directly yields the ratio of the proteins in population A versus population B. Thus, the A/B ratio reflects the quantitative changes of the protein between the two proteomes [19].

We hypothesized herein that a quantitative proteomics approach based on BST and SILAC/MS can be developed for identifying and quantifying global changes in protein SNO with simultaneous identification of the specific SNO site(s) in each SNO-protein in paired proteomes. With this method, we show that endogenous NO on VEGFA stimulation and exogenous NO from donors differentially regulates the SNO of proteins, with the VEGFA-responsive SNO targets mostly linked to endothelial cell proliferation.

MATERIALS AND METHODS

Materials

Sodium ascorbate, neocuproine, 4-(2-hydroxyethyl)-1-piperazineethanesulfonic acid (HEPES), ethylenediaminetetraacetic acid (EDTA), diethylene triamine pentaacetic acid (DTPA), copper chloride, bovine serum albumin (BSA), methanol, N-ethylmeleimide (NEM), trifluoroacetic acid, acetonitrile, and all other chemicals, unless specified, were from Sigma (St. Louis, MO). *N*-(6-[biotinamido] hexyl)-3′-(2′-pyridyldithio) propionamide (biotin-HPDP) was from Thermo Scientific (Rockford, IL). S-nitrosoglutathione (GSNO) was from Cayman (Ann Arbor, MI). Sequencing-grade trypsin was purchased from Promega Corp. (Madison, WI). SILAC RPMI-1640 (deficient in lysine and arginine) was from Invitrogen (Carlsbad, CA). L-$^{12}C_6$$^{14}N_4$-Arg, L-$^{12}C_6$$^{14}N_2$-Lys, L-$^{13}C_6$$^{15}N_4$-Arg, and L-$^{13}C_6$$^{15}N_2$-Lys were purchased from Cambridge Isotope Laboratories (Andover, MA).

Cell Isolation, Culture, and SILAC Labeling

Primary ovine fetoplacental artery endothelial cells (oFPAEC) were isolated, validated, and used in passages 6–10 as described previously [21]. The animal use protocol was approved by the Animal Subjects Committees from the University of California, San Diego, and we followed the National Research Council's Guide for the Care and Use of Laboratory Animals. For SILAC labeling, the cells were divided into two populations: one grown in SILAC RPMI-1640 medium supplemented with L-$^{12}C_6$$^{14}N_4$-Arg and L-$^{12}C_6$$^{14}N_2$-Lys (light medium containing natural isotopes) and the other in SILAC medium supplemented with L-$^{13}C_6$$^{15}N_4$-Arg and L-$^{13}C_6$$^{15}N_2$-Lys

(heavy medium containing stable isotopes). Both light and heavy media were supplemented with 10% dialyzed fetal bovine serum (FBS; GIBCO, Grand Island, NY) and 1% antibiotics. Cells were cultured in SILAC medium for at least three passages to achieve maximum labeling and then used for stimulation. Prior to stimulation, subconfluent (~80%) cells were cultured with SILAC medium containing 1% dialyzed FBS and 1% antibiotics overnight. Following 1 h of equilibration with fresh SILAC medium with 1% dialyzed FBS and 1% antibiotics, the cells were treated with VEGFA or an NO donor GSNO for up to 2 h. In this study, 10 ng/ml VEGFA was used based on our previous studies showing that VEGFA consistently stimulates in vitro angiogenesis of placental artery endothelial cells at least partially mediated by endogenously produced NO via NOS3 activation, without any notable negative effects up to 50 ng/ml [22, 23]. A relatively high level of endogenous *trans*-nitrosylating agent GSNO was used as an NO donor, which has been widely reported [24–26], for pharmacological comparison of exogenous NO. Cell lysates were prepared in a nondenaturing buffer [27] containing 1% protease inhibitor cocktail, and protein concentration was determined by the BCA Protein Assay Kit (Pierce, Rockford, IL).

SDS-PAGE and In-Gel Digestion

Protein samples were dissolved in SDS sample buffer and separated by 10%–12% SDS-PAGE, and bands of interest were cut out and digested in gel as previously described [28]. Briefly, minced gel pieces were washed with 25 mmol/L NH_4HCO_3 in 50% acetonitrile, dried in a Speedvac, and then rehydrated in 25 mmol/L NH_4HCO_3 solution containing trypsin. After overnight digestion at 37°C, the peptides were extracted with HPLC-grade water once, followed with 5% formic acid/50% acetonitrile three times. The combined supernatants were dried by Speedvac and then dissolved in 2% formic acid/3% acetonitrile. Peptides were stored at −20°C until LC-MS/MS was performed.

BST [16]

The oFPAEC cells (~1×10^6) were treated with or without VEGFA/GSNO for 30 min. Equal amounts (0.5 mg/group) of proteins from VEGFA- or GSNO-treated light cells were mixed with that of the control heavy cells. Protein content of the mixtures was redetermined and then adjusted to 0.6 mg/ml protein in a blocking buffer (250 mmol/L HEPES, pH 7.7, 1 mmol/L DTPA, 0.1 mmol/L neocuproine, 50 mmol/L NEM, and 2.5% SDS). After blocking by incubation in dark at 50°C for 30 min, the proteins were precipitated by incubation with acetone (1:3, vol/vol) at −20°C for 2 h and washed with cold acetone (70%) once. The precipitated proteins were resuspended in a labeling buffer (25 mmol/L HEPES, pH 7.7, 30 mmol/L sodium ascorbate, 0.1 μmol/L $CuCl_2$, 0.4 mmol/L biotin-HPDP, and 1% SDS); readjusted to 0.6 mg/ml; and then incubated in the dark at 37°C for 1 h with occasional agitation. The biotinylated samples were then acetone precipitated again to remove excess biotin-HPDP.

Avidin Capture of SNO-Proteins and Immunoblotting

Total biotinylated SNO-proteins were captured by incubation with 50 μl of NeutrAvidin protein-coated beads (Thermo Scientific) at 4°C overnight. The avidin-captured SNO-proteins were eluted from the beads with SDS sample buffer (100 μl) containing 100 mmol/L 2-mercaptoethenol at 37°C for 20 min. Protein samples were separated by 10%–12% SDS-PAGE and then transferred onto polyvinylidene fluoride membranes for immunoblotting with specific antibodies as previously described [21]. Anti-cofilin-1 (CFL1) antibody was from Abcam (San Francisco, CA). Anti-β-actin monoclonal antibody (1:10 000) was from Ambion (Austin, TX). Antibodies against heat shock protein-70 (HSP70, 1:500) and glyceraldehyde 3-phosphate dehydrogenase (GAPDH, 1:500) were obtained from Santa Cruz Biotechnology (Santa Cruz, CA). Band intensity was quantified by multiplying the absorbance of the surface areas using the NIH ImageJ.

Trypsin Digestion and SNO-Peptide Purification

Following BST labeling, the acetone-precipitated protein samples (1 mg/mixture) were thoroughly dissolved in 200 μl of digestion buffer (50 mmol/L NH_4HCO_3, 1 M urea) containing 20 μg of trypsin. After trypsin digestion at 37°C overnight, the samples were incubated with 50 μl of NeutrAvidin protein-coated beads at room temperature for 2 h for capturing the biotinylated SNO-peptides as described previously [29]. The SNO-peptides were eluted from the beads with 100 μl of 0.4% trifluoroacetic acid in 30% acetonitrile and then stored at −20°C until LC-MS/MS was performed. For LC-MS, 5 μg of SNO-peptides were loaded in each mass spec analysis.

LC-MS/MS Analysis and SNO-Peptide Identification

LC-MS/MS analysis of the purified SNO-peptides was performed by using an LTQ-Orbitrap XL MS (Thermo Scientific) coupled with an Eksigent NanoLC system (Eksigent, Dublin, CA), exactly as previously described [29]. The LC analysis was performed using a capillary column (100-μm inner diameter × 150 mm long) packed with C18 resins (GL Sciences, Torrance, CA), and the peptides were eluted using a linear gradient of 2%–40% B in 35 min; (solvent A: 100% H_2O/0.1% formic acid; solvent B: 100% acetonitrile/ 0.1% formic acid). A cycle of one full Fourier transform (FT) MS scan mass spectrum (350–1800 m/z, resolution of 60 000 at m/z 400) was followed by 10 data-dependent MS/MS acquired in the linear ion trap with normalized collision energy (setting of 35%). Target ions selected for MS/MS were dynamically excluded for 30 sec. Monoisotopic masses of parent ions and corresponding fragment ions, parent ion charge states, and ion intensities from LC-MS/MS spectra were extracted using in-house software based on the Raw_Extract script from Xcalibur v2.4. The data were searched using the Batch-Tag within the developmental version (v5.8.0) of Protein Prospector against a decoy database consisting of a normal Swissprot database concatenated with its randomized v9 (SwissProt.2010.03.30.random.concat with total 864 896 protein entries). The mass accuracy for parent ions and fragment ions were set as ±20 ppm and 0.8 Da, respectively. Trypsin was set as the enzyme, and the maximum of two missed cleavages were allowed. Biotin-HPDP labeling of cysteine residues was selected as constant modifications with a monoisotopic mass shift of 428.192 Da. In addition, two additional variable modifications were included: $^{13}C_6$ $^{15}N_4$-labeled arginine and $^{13}C_6$ $^{15}N_2$-labeled lysine (heavy AAs). To quantify relative protein abundance changes, the Search Compare function was used to determine the L/H ratios based on the intensities of the monoisotopic masses of the parent ion peptide pairs [30]. Search Compare also corrects for the isotopic purity of the heavy AAs, which was set to 98% purity with the signal/ noise threshold set at 10. The peptide peak intensities were averaged across the elution profile (30 sec). The proteins identified by one or two peptides were confirmed by manual inspection of the MS/MS spectra. The relative abundance ratios were also validated by the raw spectra. If two or more *S*-nitrosylation sites were identified for a specific SNO-protein, the final ratio was calculated as the average of ratios of all *S*-nitrosylation peptides for the protein.

Bioinformatics Analysis

Ingenuity pathway analysis (IPA; http://www.ingenuity.com) was used to obtain information regarding relationships, biological mechanisms, functions, and pathways of differentially regulated SNO-proteins. All differentially regulated SNO-proteins (focus molecules) with their corresponding Swiss-Prot accession numbers and fold change were imported into the IPA. Nodal molecules are those that were not identified but were found in the IPA to be either potential targets or related molecules to the identified molecules. The randomness of a biological function or network obtained by IPA is determined by calculating the P value using the Fischer exact test. The P value represents that the likelihood association between the set of the identified SNO-proteins, and a given process or pathway is due to random chance. The score of each network is a numerical value to approximate the degree of relevance and size of a network to the molecules in the given data set. The network is considered to be significant if the score is >2. The identified SNO-proteins were further classified in the UniProt knowledge database for searching their functions.

Experimental Replication and Statistical Analysis

All experiments were repeated at least three times using cells from different animals. Data were presented as mean ± SEM. Statistical analysis was performed by one-way ANOVA, followed by the Student-Newman-Keuls test for multiple comparisons using SigmaStat 3.5 (Systat Software Inc., San Jose, CA). Significant difference was defined as $P < 0.05$.

RESULTS

Effects of VEGFA and GSNO on Protein SNO in Endothelial Cells

To determine the effects of VEGFA and GSNO on protein SNO in endothelial cells, we first measured total levels of SNO-proteins in oFPAEC treated with or without VEGFA (10 ng/ml) or an NO donor GSNO (1 mM) for up to 2 h. In VEGFA-treated cells, total levels of SNO-proteins began to increase at 10 min, maximized around 30 min, and returned to baseline at 60 min (Fig. 1). In GSNO-treated cells, total levels

of SNO-proteins began to increase at 10 min, reached levels comparable to maximal response to VEGFA at around 30 min, and continued to increase at least 2 h. In keeping with our recent studies showing that endogenous NO derived from NOS3 mediates VEGFA stimulation of protein SNO in endothelial cells [31], the different SNO time courses demonstrate that endogenous NO on VEGFA stimulation and exogenous NO from GSNO differentially stimulate endothelial protein SNO.

Development of a Quantitative Nitroso-*Proteomics Method Using BST, SILAC, and LC-MS/MS*

The strategy of SILAC/BST-based quantitative *nitroso*-proteomics analysis method is shown schematically in Figure 2. In this method, a mass difference was introduced between the control and VEGFA/GSNO-treated cells to identify and quantify SNO via MS. Two populations of cells were labeled with light (L-$^{12}C_6$ $^{14}N_4$-Arg and L-$^{12}C_6$ $^{14}N_2$-Lys) and heavy (L-$^{13}C_6$ $^{15}N_4$-Arg and L-$^{13}C_6$ $^{15}N_2$-Lys) isotopes, respectively. The cells were cultured with the light and heavy AAs separately for more than three passages to reach saturated labeling. Similar to previous reports [32, 33] showing that isotope labeling had no influence on cell growth and properties, oFPAEC seemed to proliferate and grow morphologically normal, as the two groups of cells did not differ significantly after four passages in the SILAC labeling medium containing light or heavy AAs. As determined by LC-MS/MS (Fig. 3), the incorporation of heavy AAs continuously increased with passage and saturated at a plateau rate of ~98% after four passages.

The heavy cells (H) were used as the control to avoid possible excess utilization of arginine by NOS3 during NO synthesis [34]. The light cells were used for treatment with 10 ng/ml VEGFA (L1) or 1 mM GSNO (L2). Treatments with both VEGFA and GSNO induced comparable significant SNO responses at 30 min; thereafter, the VEGFA response declined, and the GSNO response continued to increase (Fig. 1). These data suggest that at this time point, VEGFA and GSNO stimulates the most common SNO-protein targets of functional significance. Thirty minutes of treatment was therefore chosen for analyzing the differential VEGFA and GSNO-responsive SNO-proteins. Following treatment, both cell populations were harvested and lysed. Equal amounts of proteins from group L1 or L2 were mixed with H; the mixtures (i.e., L1/H and L2/H) were subjected to BST and trypsin digestion. The biotinylated peptides (SNO-peptides) were affinity purified and then identified by MS. If an SNO-protein is present in the samples, the resulting Arg/Lys-containing peptides will be observed as pairs with heavy or light AAs originated from the incorporated isotopes. The abundance of SNO-proteins in the two groups could be quantified according to the ratios of the peak intensities of the paired Arg/Lys peptides determined by LC-MS/MS (i.e., R1 = L1/H and R2 = L2/H). Peptides derived from the proteins present in only one sample and peptides containing no arginine/lysine were observed as a singlet in the LC-MS spectra; however, these peptides were nitrosylated as well since only SNO-peptides were purified for LC-MS/MS.

Comparisons of the Common and VEGFA- or GSNO-Responsive Nitroso-*Proteomes*

Although both endogenous NO on VEGFA stimulation and exogenous NO from donors stimulate placental endothelial cell proliferation [35], endogenous NO on estradiol-17β stimulation and exogenous NO from donors differentially regulate
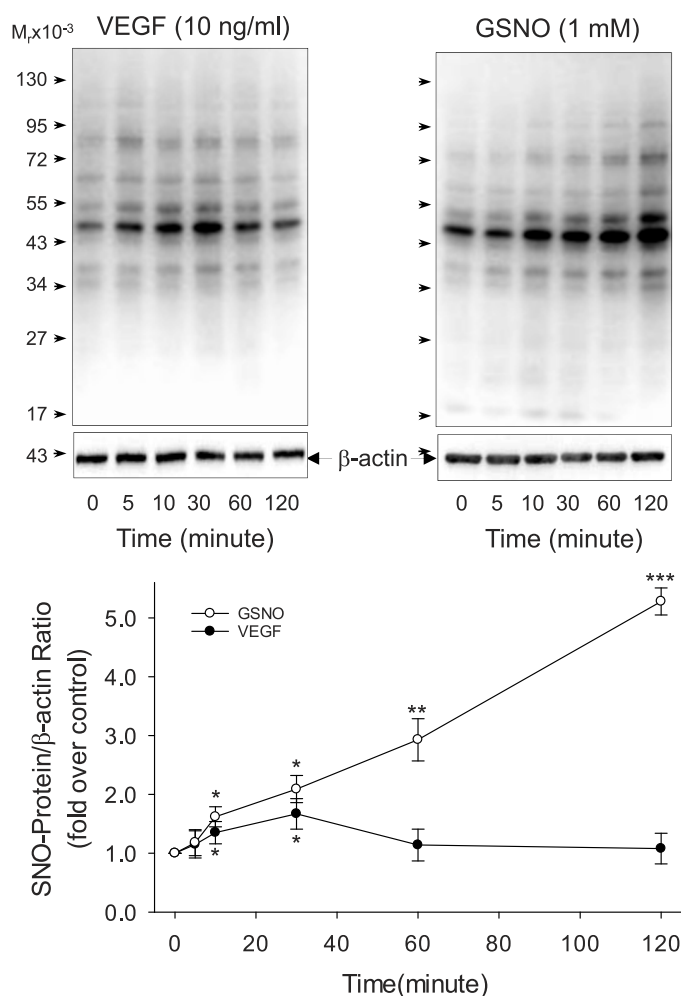
FIG. 1. Time courses of VEGFA- and GSNO-induced endothelial protein *S*-nitrosylation. Subconfluent cells were treated with or without 10 ng/ml VEGFA or 1 mM GSNO for the indicated times. Total protein extracts were harvested for determining total SNO-proteins. Representative blots of total SNO-proteins and β-actin of one typical experiment are shown. Lower graphs summarize data (mean ± SEM, n = 3) from three independent experiments using cells from different animals. *$P < 0.05$, **$P < 0.01$, and ***$P < 0.001$ vs. control.

FIG. 2. Schematic overview of BST SILAC and LC-MS/MS assay. Cells were labeled with light or heavy isotope-labeled amino acids. Light isotope-labeled cells were treated with VEGFA or GSNO (treatment group, L1 or L2), and heavy isotope-labeled cells were used as control group (H). Equal amounts of cell lysates from treatment and control groups were mixed for labeling SNO-proteins by BST. After tryptic digestion, the biotinylated SNO-peptides were purified by Avidin Capture and then analyzed by LC-MS/MS for protein identification. The spectral data of each paired SNO-peptides were used to calculate the ratios (L1/H and L2/H) that give the quantitative responses to treatments.

mitochondrial SNO in human umbilical cord vein endothelial cells [29]. Thus, it is possible that endogenous NO on VEGFA stimulation and exogenous NO from donors might affect common and different proteins via SNO. We then analyzed the *nitroso*-proteomes of the control and VEGFA- and GSNO-treated oFPAEC by the quantitative proteomics method using BST, SILAC, and LC-MS/MS as illustrated in Figure 2.

After a database search, proteins with unique cysteine-containing SILAC pair(s) were used as a criterion for identifying SNO-proteins. A total of 387 SNO-peptide pairs were identified; there were overlaps in the mixtures of VEGFA/control (L1/H) and GSNO/control (L2/H) samples, including 72 exclusively present in former, 127 only in the later, and 188 in both groups. As a result, a total of 213 SNO-proteins were confidently identified, including 27 in L1/H, 61 in L2/H, and 125 in both groups.

The Search Compare program within the developmental version of Protein Prospector was used to calculate the relative abundance ratios of Arg/Lys-containing peptides based on ion intensities of monoisotopic peaks observed in the LC-MS spectra when the peptides were sequenced and subsequently

identified during database searching. For instance, in the SILAC peptide MAASCILLHTGQK from alcohol dehydrogenase [NADP+] (AKR1A1, Q3ZCJ2) in the GSNO-treated group, the three left peaks shown in Figure 4 are the MS signals of light isotope-labeled peptides. The heavy isotope-labeled peptides on the right have a +4 m/z shift because there is a Lys in these peptides, and L-$^{13}C_6$$^{15}N_2$-Lys is +8 Da heavier in mass compared to L-$^{12}C_6$$^{14}N_2$-Lys. Based on the intensity of the peaks, the ratio of L/H was calculated as 2.64. Since MAASCILLHTGQK is the only cysteine-containing SILAC peptide identified, this result showed that the SNO of AKR1A1 increased by 2.64-fold by GSNO treatment. For proteins with multiple SILAC peptide pairs identified, the overall SNO ratio was calculated by averaging all single ratios. Based on this algorithm, the changes of all SNO-proteins were quantified and are summarized in Table 1. Based on a standard statistic power calculation (n = 3, 10% RSD, 95% confidence interval) [36, 37] and the likelihood of being able to validate a

FIG. 3.   Incorporation of stable isotope into oFPAEC. Proteins from cells grown in the medium with heavy amino acids at passages 1–6 were digested and analyzed with LC-MS/MS.

change by alternative methodology, we considered a fold change of 1.3 (or a ratio of 0.78) as a cutoff value for determining a significant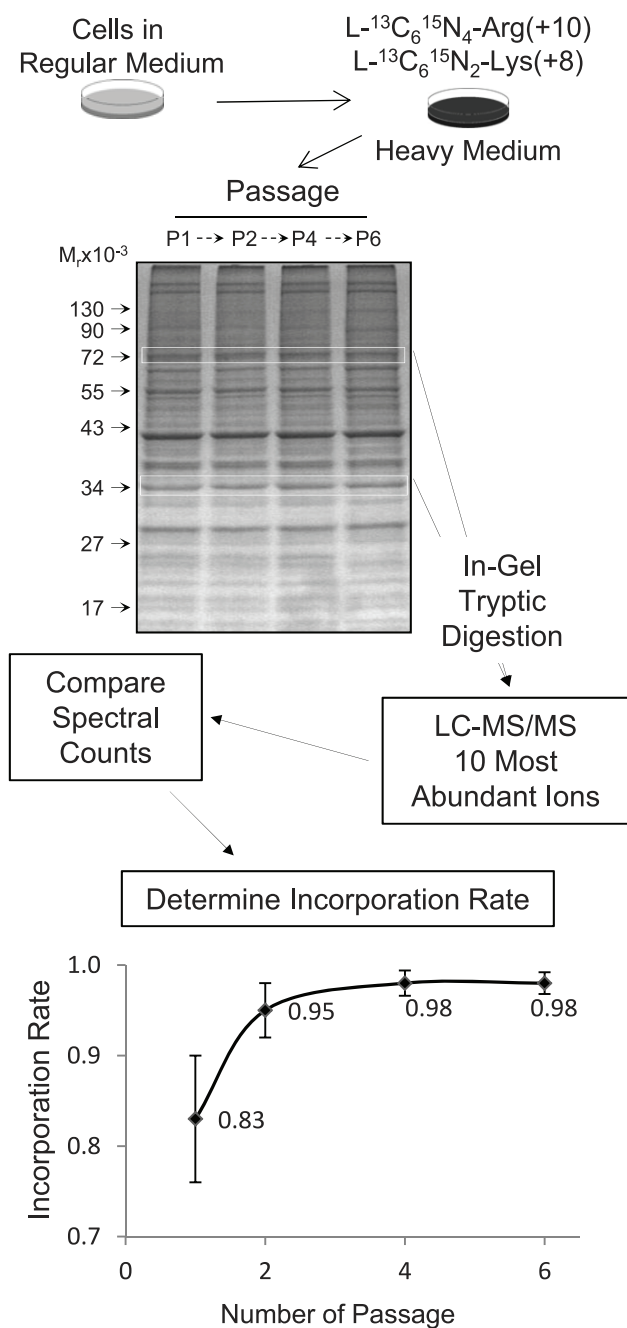 change in *S*-nitrosylation level. We found a total of 182 SNO-proteins that were identified to be responsive to treatment with VEGFA and GSNO. These included 69 that were significantly enhanced by VEGFA treatment and 94 that were significantly enhanced by GSNO treatment. Moreover, since the specific SNO site(s) were labeled with biotin by BST and only biotinylated SNO-peptides were identified by LC-MS/MS, all SNO-proteins were identified with the specific SNO site(s) simultaneously. The quantitation data were from three independent experiments using cells from different animals. The identified proteins/peptides were observed in all three runs. The mean ratio was

calculated and is listed in Table 2. For those whose *P* values were >0.05, the ratio is listed in Table 2 to indicate that the specific protein targets were detected in all three runs. For those peptides in only one or two runs, they were omitted and are listed as N/A in Table 2.

Validation of the Identified SNO-Proteins

To validate the changes of SNO-proteins identified by the quantitative proteomics method, we analyzed SNO-proteins identified to be VEGFA/GSNO-responsive SNO targets, including HSP70, GAPDH, and CFL1 in endothelial cells by immunoblotting of the purified total SNO-proteins with specific antibodies. As summarized in Figure 5, VEGFA and GSNO stimulated time-dependent changes in the SNO of each of these proteins. The VEGFA- and GSNO-induced time courses were similar with that of the total SNO responses to VEGFA and GSNO as shown in Figure 1. Both induced maximal responses at 30 min posttreatment; however, VEGFA-induced responses returns to baseline after 60 min, and the GSNO-induced response persisted at high levels up to 2 h. VEGFA stimulated SNO of HSP70, GAPDH, and CFL1 by 2.22-, 1.77-, and 1.66-fold at 30 min, respectively, whereas GSNO stimulated SNO of HSP70, GAPDH, and CFL1 by 2.47-, 2.79-, and 2.55-fold, respectively. These changes were comparable to those summarized in Table 2; VEGFA stimulated SNO of HSP70, GAPDH, and CFL1 by 2.14-, 1.31-, and 2.01-fold at 30 min, respectively, whereas GSNO stimulated SNO of HSP70, GAPDH, and CFL1 by 2.58-, 2.78-, and 2.68-fold, respectively.

Bioinformatics Analysis

Functional analysis suggested that the SNO-proteins are associated with various functions, including cell cycle and proliferation, cytoskeleton and motility, metabolism, protein synthase and modification, and cellular signaling and transportation (Fig. 6). The biological function analysis indicates that EIF2 signaling is the most significant signaling pathway for both VEGFA- and GSNO-responsive SNO-proteins, with 22 and 25 focus molecules and a −lg (*P* value) of 20.1 and 21.5, respectively (Table 1). Gene expression/protein synthesis was identified as the TOP 1 molecular and cellular function for the VEGFA- and GSNO-responsive SNO-proteins, with the most significant network analysis score of 64, representing 31 focus molecules (Fig. 7).

DISCUSSION

In the present study, we have successfully developed a quantitative proteomics approach for analyzing global protein SNO in paired proteomes by using BST, SILAC, and LC-MS/MS. With this high-throughput approach, we show herein for the first time that endogenous NO via NOS3 activation on VEGFA stimulation and a widely used NO donor GSNO [24–26] regulate common and different target proteins through SNO, with the VEGFA-responsive SNO targets mostly linked to endothelial cell proliferation. Because endothelial NOS3-derived NO plays a key role in mediating VEGF-stimulated angiogenesis [2–4] and our recent studies showing that VEGFA stimulates SNO via NOS3-derived NO in endothelial cells [31, 38], the VEGFA-responsive endothelial SNO-proteins identified herein provide a fundamental database for future functional analysis of SNO in regulating endothelial cell biology on VEGFA stimulation, especially as it pertains to angiogenesis.
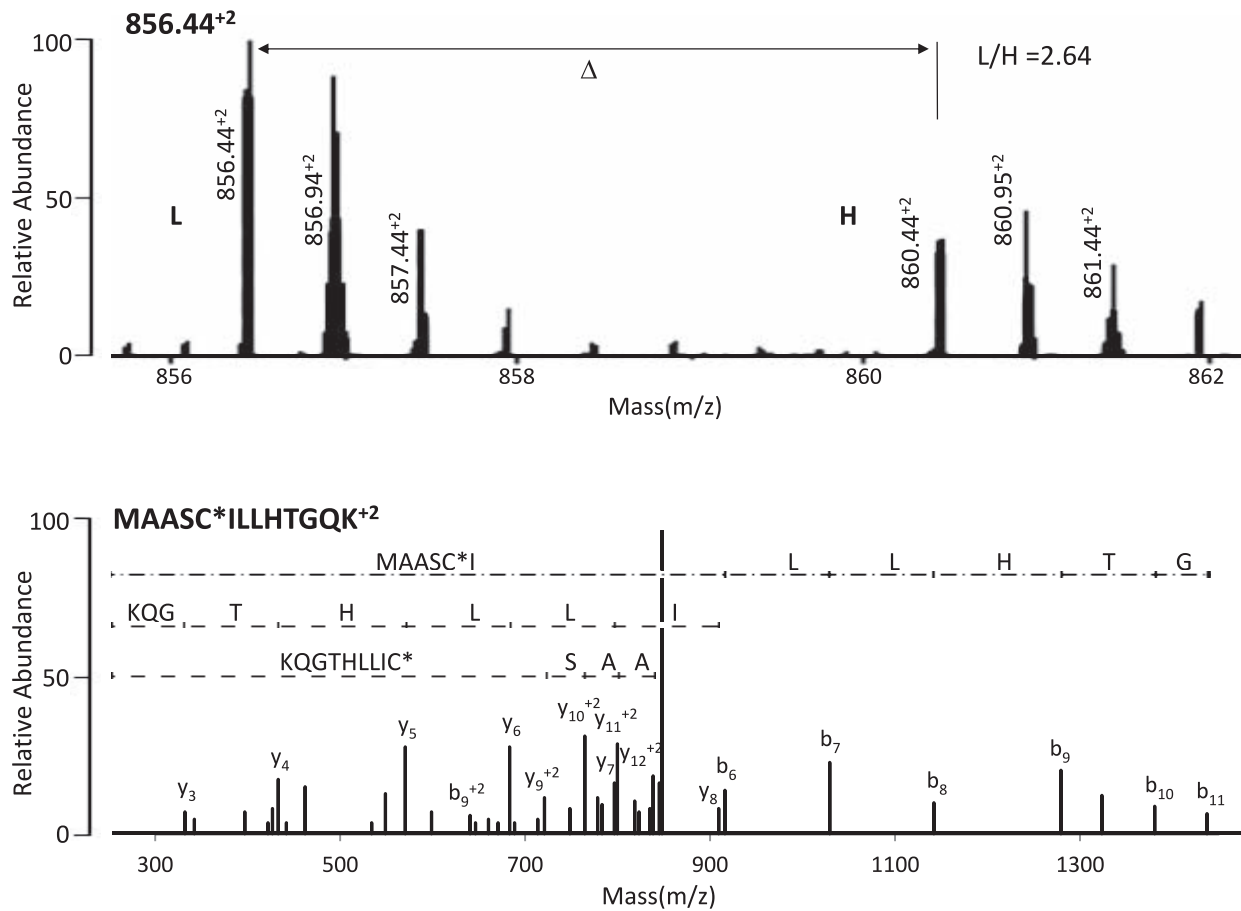
FIG. 4. Quantification and identification of SNO peptides. Comparison of light and heavy reagent elution profiles for the alcohol dehydrogenase peptide MAASCILLHTGQK.

VEGFA is the primary angiogenic factor whose role in angiogenesis has been well documented to be mediated mainly by NO produced by NOS3 activation [2–4]. We have shown that endogenous NO derived from NOS3 is critical for mediating VEGFA-induced placental endothelial cell angiogenesis [21, 39, 40], and exogenous NO from donors also stimulates placental endothelial cell proliferation [35]. We also have shown that activation of mitogen-activated protein kinases and protein kinase B/Akt pathways is important for both VEGFA-stimulated placental endothelial proliferation [35, 41] and gene expression [42]. Although these signaling pathways are downstream of NOS3-NO in mediating VEG-FA-induced placental angiogenesis, they seem not to be regulated by NO directly.

SNO has been increasingly recognized as a critical NO signaling mechanism for NO to directly regulate protein function to participate in nearly all major categories of biological pathways [6]. For instance, we have recently shown that VEGFA and estradiol-17β stimulates dynamic SNO of proteins in endothelial cells, which are linked to a variety of biological functions [31, 38]. We have recently shown that SNO of CFL1 on different cysteines have different functions in response to different extracellular stimuli. SNO on Cys80/139 results in increased actin-severing activity of CFL1, which mediates VEGFA-stimulated endothelial cytoskeleton remod-

TABLE 1. Ingenuity pathway analysis of nitroso-proteomes.*

Pathways	VEGF			GSNO		
	−lg (P value)	No. of molecules	Overlap	−lg (P value)	No. of molecules	Overlap
Canonical pathways						
EIF2 signaling	20.1	22	11.7%	21.5	25	13.5%
Epithelial adherens junction signaling	10.4	13	8.8%	11.3	15	10.3%
Remodeling of epithelial adherens junctions	10.4	10	14.7%	12.0	12	17.6%
Molecular and cellular functions						
Protein synthesis	13.0–3.3	40	N/A	14.1–3.3	45	N/A
Cell death and survival	14.1–2.4	81	N/A	13.2–2.5	88	N/A
Cellular growth and proliferation	16.6–2.7	88	N/A	10.7–2.7	88	N/A

* Signaling pathways and molecular functions were analyzed by the Ingenuity Pathway Analysis software. The calculations are based on the VEGF- and GSNO-responsive protein sets, respectively. The column "Overlap" was used to describe the percentage of known components existing in the VEGF- and GSNO-responsive protein sets, respectively, against the total components of each individual classical canonical pathway. N/A, not detected.
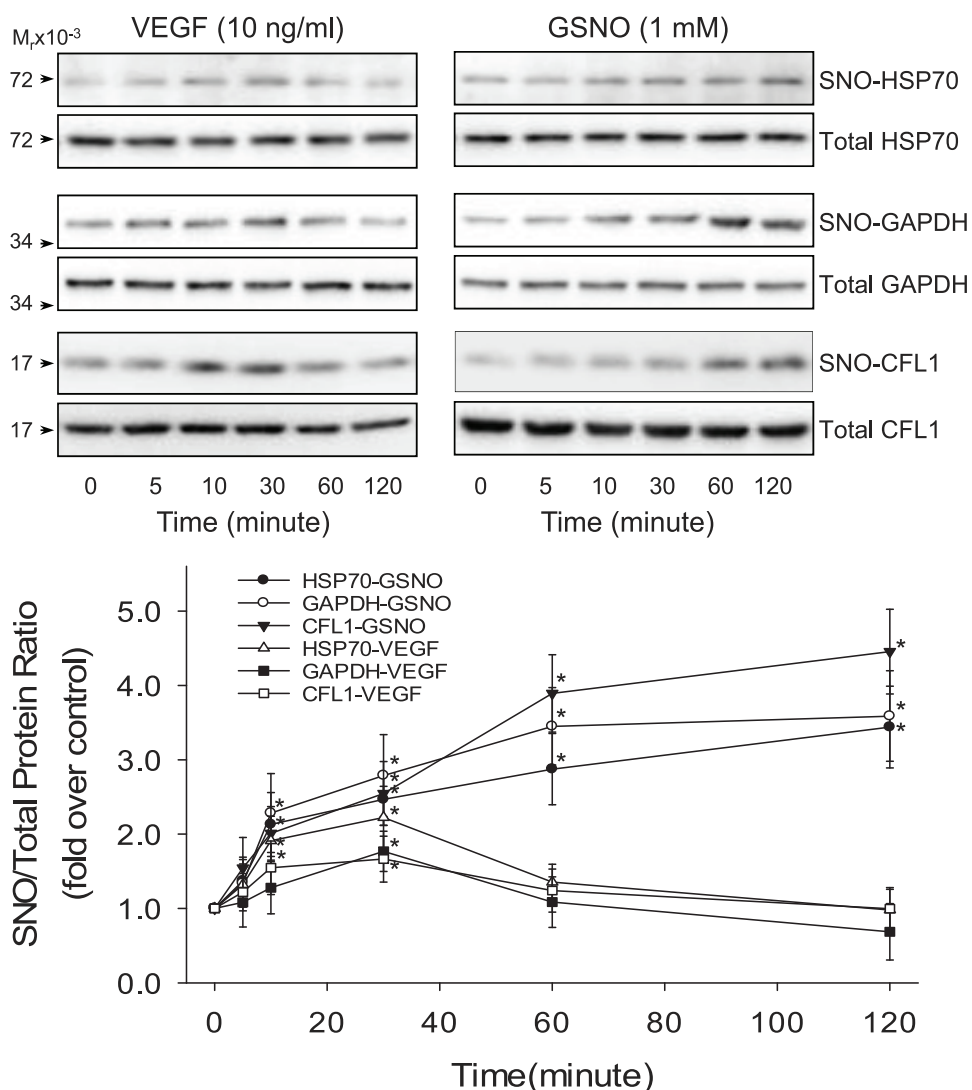
FIG. 5. Time courses of specific endothelial SNO-proteins in response to stimulation with VEGFA and GSNO. Cells were treated with VEGFA or GSNO for up to 2 h. Whole cell lysates were prepared for labeling SNO-proteins by BST. The biotinylated SNO-proteins were captured by avidin-coated beads for analyzing total and nitrosylated HSP70, GAPDH, and CFL1 by immunoblotting with specific antibodies, respectively. Lower graphs summarize data (mean ± SEM, n = 3) from three independent experiments using oFPAEC from different animals. *P < 0.05 versus control.

eling and cell migration [31]. However, on estrogen stimulation, SNO of CFL1 occurs primarily on Cys80, which in turn mediates estrogen stimulation of cytoskeleton remodeling in endothelial cells [38]. Thus, our findings have further highlighted the importance of identification of the specific SNO sites for delineating the mechanism by which SNO regulates endothelial cell function in response to stimulation.

As a posttranslational modification of proteins on specific cysteine residues, SNO is capable of affecting the proteome of a cell. Similar to *O*-phosphorylation and other posttranslational modifications [7], SNO occurs only on specific cysteine residues with a specific surrounding sequence [6]. Thus, identification of the specific SNO sites (reactive cysteines) is a prerequisite for subsequently deciphering the functional consequences of SNO of a specific protein. However, the detection of SNO used to be troublesome because of its low level and liability. Antibodies directed against the SNO functionality have suffered from a lack of specificity and loss of sensitivity during immunodetection, as the S-NO bond is sensitive to redox changes even in in vitro assays [43, 44]. The invention of a reliable and reproducible BST for measuring

SNO in 2001 [15] has greatly accelerated the understanding of protein SNO in biology and medicine, exemplified by an explosion of more than 1500 publications on this topic to date. The three-step BST method selectively converts the S-NO groups into stable biotinylated ones, allowing SNO-proteins to be readily displayed, affinity purified, and identified [15]. According to this principle, many modified BST methods have been developed. For instance, replacing the biotin tag with fluorescence tags [45] allows the SNO-proteins to be detected in cells/tissues in situ [16, 46]. We have reported a proteomics approach for analyzing SNO-proteins from paired proteomes by labeling them with two different fluorescently labeled tags and 2D-DIGE/MALDI-TOF/MS; this method allows identifying partial *nitroso*-proteomes in endothelial cells and human placentas and relatively quantifying changes in endothelial protein SNO in response to estrogen and placental SNO under the influence of preeclampsia [14, 16, 17]. Others also have developed different proteomics approaches based on BST for analyzing protein SNO [47–49]. Although the proteomics approaches reported to date have provided insightful databases of SNO-proteins in various tissues/cells and greatly accelerated

TABLE 2. The *nitroso*-proteomes in VEGF- or GSNO-treated ovine fetoplacental artery endothelial cells identified by BST-SILAC mass spectrometry.

ID	Protein name	Ratio to control[a]		SNO-peptides identified[a]	
		VEGF	GSNO	VEGF	GSNO
Cell cycle and proliferation					
Q27971	Calpain-2 catalytic subunit (CAPN2)	1.47*	3.05*	GSTAGGCR, MPCQLHQVIVAR, RPTEICDNPQFITGGATR	LEICNLTPDTLTSDSYK, MPCQLHQVIVAR, RPTEICDNPQFITGGATR
P04632	Calpain small subunit 1 (CAPNS1)	1.54*	2.23*	TDGFGIDTCR	TDGFGIDTCR
P81184	Galectin-1 (LGALS1)	1.90*	2.64*	DDNNLCLHFNPR, FNAHGDVNTIVCNSK, MACGLVASNLNLKPGEC§LR	DDNNLCLHFNPR, FNAHGDVNTIVCNSK, MACGLVASNLNLKPGEC§LR
Q15366	Poly(rC)-binding protein 2 (PCBP2)	2.13*	2.72*	AITIAGIPQSIIECVK, INISEGNCPER, LVVPASQCGSLIGK	INISEGNCPER, LVVPASQCGSLIGK
P62826	GTP-binding nuclear protein Ran (RAN)	1.47	2.15*	VCENIPIVLC§GNK	VC§ENIPIVLC§GNK
P31949	Protein S100-A11(S100A11)	1.74	2.99	CIESLIAVFQK	CIESLIAVFQK
P61981	14-3-3 protein gamma (YWHAG)	1.54	2.79	NCSETQYESK	NCSETQYESK
P29361	14-3-3 protein zeta/delta (YWHAZ)	1.52*	2.52*	ACSLAK, DICNDVLSLLEK, YDDMAACMK	ACSLAK, DICNDVLSLLEK, YDDMAACMK
O43684	Mitotic checkpoint protein BUB3 (BUB3)	N/A	7.09	N/A	TPCNAGTFSQPEK
Q53EL6	Programmed cell death protein 4 (PDCD4)	N/A	6.41	N/A	AVGDGILCNTYIDSYK
P36873	Serine/threonine-protein phosphatase PP1-gamma catalytic subunit (PPP1CC)	N/A	3.23*	N/A	GNHECASINR, IFCCHGGLSPDLQSMEQIR‡
P62262	14-3-3 protein epsilon (YWHAE)	N/A	4.98	N/A	LICCDILDVLDK
Q12906	Interleukin enhancer-binding factor 3 (ILF3)	1.33	N/A	CLAALASLR	N/A
P33992	DNA replication licensing factor MCM5 (MCM5)	6.84	N/A	CPLDPYFIMPDK	N/A
P68509	14-3-3 protein eta (YWHAH)	1.35	N/A	NCNDFQYESK	N/A
P27348	14-3-3 protein theta (YWHAQ)	3.18	N/A	YLAEVACGDDR	N/A
Cytoskeleton and motility					
P60713	Actin, cytoplasmic 1 (ACTB)	2.65*	4.08*	CDVDIR, CDVDIRK, MDDDIAALVVDNGSGMCK	CDVDIR, CDVDIRK, CPEALFQPSFLGMESC§GIHETTFNSIMK, MDDDIAALVVDNGSGMCK
P63258	Actin, cytoplasmic 2 (ACTG)	3.08*	4.22*	MEEEIAALVIDNGSGMCK	CPEALFQPSFLGMESC§GIHETTFNSIMK, MEEEIAALVIDNGSGMCK
Q3B7N2	Alpha-actinin-1 (ACTN1)	2.81*	5.53*	DGLGFCALIHR, ICDQWDNLGALTQK	CQLEINFNTLQTK, ICDQWDNLGALTQK, MVSDINNAWGCLEQAEK, TFTAWCNSHLR
A5D7D1	Alpha-actinin-4 (ACTN4)	3.58*	6.23*	CQLEINFNTLQTK, ELPPDQAEYCIAR, ICDQWDALGSLTHSR, TFTAWCNSHLR	CQLEINFNTLQTK, ICDQWDALGSLTHSR, TFTAWCNSHLR
P61157	Actin-related protein 3 (ACTR3)	0.84	2.07*	DYEEIGPSICR, LPAC§VVDC§GTGYTK, YSYVCPDLVK	DYEEIGPSICR, LPACVVDCGTGYTK, YSYVCPDLVK
O15144	Actin related protein 2/3 complex subunit2 (ARPC2)	1.39	2.14	NCFASVFEK	NCFASVFEK
Q35YV4	Adenylyl cyclase-associated protein 1 (CAP1)	3.60*	5.92*	LEAVSHASDTHCGYGDSAAK, NSLDCEIVSAK	ALLVTASQCQQPAGNK, LEAVSHASDTHCGYGDSAAK
Q6B7M7	Cofilin-1 (CFL1)	2.01*	2.68*	HELQANCYEEVKDR	AVLFCLSEDKK, CTLAEK, HELQANCYEEVKDR, MLPDKDCR
Q0VFX8	Cysteinerich protein2 (CRIP2)	1.64	4.09	ASSVTTFTGEPNMCPR	ASSVTTFTGEPNMCPR
P60981	Destrin (DSTN)	1.72*	3.37*	HECQANGPEDLNR, KCSTPEEIK	HECQANGPEDLNR
P21333	Filamin-A (FLNA)	1.75*	3.75	MDC§QECPEGYR, SSFTVDCSK	MDC§QECPEGYR
O75369	Filamin-B (FLNB)	2.67*	4.30*	APSVATVGSICDLNLK, CLATGPGIASTVK, GAGTGGLGLTVEGPCEAK, IEYNDQNDGSCDVK, MDCQETPEGYK, MDGTYACSYTPVK, VAVTEGCQPSR, VDIQTEDLEDGTCK, SSTETCYSAIPK, SSFLVDCSK	APSVATVGSICDLNLK, CLATGPGIASTVK, GAGTGGLGLTVEGPCEAK, IEYNDQNDGSCDVK, MDCQETPEGYK, MDGTYACSYTPVK, VDIQTEDLEDGTCK, VAVTEGCQPSR, SGCIVNNLAEFTVDPK, SPFVVQVGEACNPNACR,
Q16658	Fascin (FSCN1)	1.69*	2.13*	GEHGFIGCR, LSCFAQTVSPAEK	GEHGFIGCR, LSCFAQTVSPAEK

TABLE 2. *Continued.*

ID	Protein name	Ratio to control[a] VEGF	Ratio to control[a] GSNO	SNO-peptides identified[a] VEGF	SNO-peptides identified[a] GSNO
Q3B7M5	LIM and SH3 domain protein 1 (LASP1)	3.51	4.02	MGPSGGEGLECER	MGPSGGEGLECER
P02545	Lamin-A/C (LMNA)	1.53*	2.37*	AQNTWGCGNSLR, TVLCGTC§GTCGQPADK	AQNTWGCGNSLR, TVLCGTC§GQPADK
P35579	Myosin-9 (MYH9)	1.82*	2.93*	ADFCIIHYAGK, CNGVLEGIR, CQHLQAEK, EDQSILCTGESGAGK, SMMQDREDQSILCTGESGAGK, CIIPNHEK	ADFCIIHYAGK, CNGVLEGIR, CQHLQAEK, EDQSILCTGESGAGK, SMMQDREDQSILCTGESGAGK, VEDMAELTCLNEASVLHNLK
P60660	Myosin light polypeptide 6 (MYL6)	1.79*	2.04	ILYSQCGDVMR, MCDFTEDQTAEFK	ILYSQCGDVMR
Q96HC4	PDZ and LIM domain protein 5 (PDLIM5)	0.959	1.48*	GCTGSLNMTLQR	GCTGSLNMTLQR
Q13813	Spectrin alpha chain (SPTAN1)	8.91	3.72*	DCEQAENWMAAR	ALCAEADR, DCEQAENWMAAR, GACAGSEDAVK
Q01082	Spectrin beta chain (SPTBN1)	1.98*	3.05	FATDGEGYKPCDPQVIR, IHCLENVDK	IHCLENVDK
P81947	Tubulin alpha-1B chain (TUBA1B)	1.36*	2.48*	SIQFVDWCPTGFK, YMACC§LLYR	AYHEQLSVAEITNACFEPANQMVK, SIQFVDWCPTGFK, YMACC§LLYR
Q2HJ86	Tubulin alpha-1D chain (TUBA1D)	1.32*	2.46*	TIQFVDWCPTGFK, YMACC§LLYR	AYHEQLSVAEITNACFEPANQMVK, TIQFVDWCPTGFK, YMACC§LLYR
P04350	Tubulin beta-4 chain (TUBB4A)	1.95*	3.34*	LTTPTYGDLNHLVSATMSGVTTCLR, TAVCDIPPR	EAESCDCLQGFQLTHSLGGGTGSGMGTLLISK‡, EIVHLQAGQCGNQIGAK, LTTPTYGDLNHLVSATMSGVTTCLR, NMMAACDPR
P48616	Vimentin (VIM)	2.50*	2.73*	QVQTLTCEVDALK, QVQTLTCEVDALKGTNESLER	QVQTLTCEVDALK, RQVQTLTCEVDALK, QVQTLTCEVDALKGTNESLER
A7MB62	Actin-related protein 2 (ACTR2)	N/A	2.44*	N/A	KVVVCDNGTGFVK, LCYVGYNIEQEQK
Q15417	Calponin-3 (CNN3)	N/A	2.87*	N/A	CASQAGMTAYGTR
Q9ULV4	Coronin-1C (CORO1C)	N/A	2.70*	N/A	KCEPIIMTVPR, SIKDTICNQDER
Q14247	Src substrate cortactin (CTTN)	N/A	1.38*	N/A	HCSQVDSVR
P61285	Dynein light chain 1, cytoplasmic (DYNLL1)	N/A	7.41*	N/A	NADMSEEMQQDSVECATQALEK, YNPTWHCIVGR
O94832	Myosin-Id (MYO1D)	N/A	1.91	N/A	HLQVNVTNPVQCSLHGK
Q5E9E1	PDZ and LIM domain protein 1 (PDLIM1)	N/A	1.75	N/A	GCTDNMTLTVAR
Q9Y490	Talin-1 (TLN1)	N/A	2.99	N/A	NCGQMSEIEAK
Q05B47	Tubulin alpha-4A chain (TUBA4A)	N/A	2.48*	N/A	AYHEQLSVAEITNACFEPANQMVK, SIQFVDWCPTGFK, YMACC§LLYR
Q05B49	Tubulin beta-6 chain (TUBB6)	N/A	2.61*	N/A	EIVHIQAGQCGNQIGTK, NMMAACDPR
Q05B51	WD repeat-containing protein 1 (WDR1)	N/A	4.43	N/A	MTVDEHGQLVSCSMDDTVR
P47756	F-actin-capping protein subunit beta (CAPZB)	2.89	N/A	MSDQQLDCALDLMR	N/A
P21291	Cysteine and glycine-rich protein 1 (CSRP1)	1.86	N/A	CSQAVYAAEK	N/A
P20700	Lamin-B1 (LMNB1)	2.24	N/A	CQSLTEDLEFR	N/A
A7E3Q8	Plastin-3 (PLS3)	1.65*	N/A	KLENCNYAVELGK	N/A
Q5E9F5	Transgelin-2 (TAGLN2)	3.61	N/A	DGTVLCELINGLYPEGQAPVKK	N/A
Q05B48	Tubulin beta-3 chain (TUBB3)	1.77*	N/A	EIVHIQAGQCGNQIGAK, NMMAACDPR	N/A
Metabolism					
Q3ZCJ2	Alcohol dehydrogenase [NADP+] (AKR1A1)	1.64*	2.64	MAASCILLHTGQK	MAASCILLHTGQK
P49419	Alpha-aminoadipic semialdehyde dehydrogenase (ALDH7A1)	4.75	21.2	GEVITTYCPANNEPIAR	GEVITTYCPANNEPIAR
P04075	Fructose-bisphosphate aldolase A (ALDOA)	3.88*	5.63*	ALANSLACQGK, YASICQQNGIVPIVEPEILPDGDHDLKR	ALANSLACQGK, ALSDHHIYLEGTLLKPNMVTPGHACTQK
A2SW69	Annexin A2 (ANXA2)	1.8*	2.34*	ALLYLCGGDD, GLGTDEDSLIEIICSR, MSTVHEILCK, SVCHLQK	GLGTDEDSLIEIICSR, MSTVHEILCK, SVCHLQK
P05631	ATP synthase subunit gamma, mitochondrial (ATP5C1)	1.31	2.27	GLCGAIHSSVAK	GLCGAIHSSVAK
P13620	ATP synthase subunit d, mitochondrial (ATP5H)	1.7	2.35	SCAEFLTQSK	SCAEFLTQSK
P62633	Cellular nucleic acid-binding protein (CNBP)	1.89*	4.66*	CGESGHLAR, TSEVNCYR	CGESGHLAR, C§GETGHVAINCSK, DCDHADEQK, DCDLQEDAC§YNC§GR, TSEVNCYR

TABLE 2. Continued.

ID	Protein name	Ratio to control[a]		SNO-peptides identified[a]	
		VEGF	GSNO	VEGF	GSNO
Q92841	Probable ATP-dependent RNA helicase DDX17 (DDX17)	2.23*	3.06*	CTYLVLDEADR, GDGPICLVLAPTR	CTYLVLDEADR, GDGPICLVLAPTR
Q13838	Spliceosome RNA helicase BAT1 (DDX39B)	1.88*	3.23*	HFILDECDK, NCPHIVVGTPGR	HFILDECDK, NCPHIVVGTPGR
O02675	Dihydropyrimidinase-related protein 2 (DPYSL2)	1.57	2.57	SITIANQTNCPLYITK	SITIANQTNCPLYITK
P06733	Alpha-enolase (ENO1)	1.22	2.44	SCNC$LLLK, VNQIGSVTESLQACK	VNQIGSVTESLQACK
P55052	Fatty acid-binding protein, epidermal (FABP5)	1.28	1.94*	TQTVCNFTDGALVQHQEWDGK, TTQFSCK, VGAMAKPDCIITSDGK	TTQFSCK, VGAMAKPDCIITSDGK
P10096	Glyceraldehyde-3-phosphate dehydrogenase (GAPDH)	1.31*	2.78*	IVSNASC$TTNCLAPLAK, VPTPNVSVVDLTCR	IVSNASC$TTNC§LAPLAK, VPTPNVSVVDLTCR
Q00839	Heterogeneous nuclear ribonucleoprotein U (HNRNPU)	1.41*	2.04*	KAVVVCPK	MCLFAGFQR, KAVVVCPK
P00492	Hypoxanthine-guanine phosphoribosyltransferase (HPRT1)	0.883	3.52*	SYCNDQSTGDIK	DLNHVCVISETGK, SYCNDQSTGDIK
P19858	L-lactate dehydrogenase A chain (LDHA)	1.75*	2.73*	VIGSGCNLDSAR, VTLTHEEEACLK	VIGSGCNLDSAR, VTLTHEEEACLK
Q32LG3	Malate dehydrogenase, mitochondrial (MDH2)	2.22*	3.12*	GCDVVVIPAGVPR, GYLGPEQLPDCLK, SQETDCPYFSTPLLLGK, TIIPLISQCTPK	GCDVVVIPAGVPR, GYLGPEQLPDCLK, SQETDCPYFSTPLLLGK, TIIPLISQCTPK
O00567	Nucleolar protein 56 (NOP56)	1.87*	3.87	IDCFSEVPTSVFGEK, IINDNAYCR	IDCFSEVPTSVFGEK
P06748	Nucleophosmin (NPM1)	5.88*	13.2*	MEDSMDMDMSPLRPQNYLFGCELK	MEDSMDMDMSPLRPQNYLFGCELK
P18669	Phosphoglycerate mutase 1 (PGAM1)	3.62	6.32*	YADLTEDQLPSCESLK	YADLTEDQLPSCESLK, YADLTEDQLPSCESLKDTIAR
Q3T0P6	Phosphoglycerate kinase 1 (PGK1)	2.19*	5.65	ACADPAAGSVILLENLR, YCLDSGAK	ACADPAAGSVILLENLR
Q5EAD2	D-3-phosphoglycerate dehydrogenase (PHGDH)	2.32*	10.2*	ALVNHENVISCPHLGASTK	ALQSGQCAGAALDVFTEEPPRDR, ALVNHENVISCPHLGASTK, NSGSCLAPAVIIGLLK
P14618	Pyruvate kinase isozymes M1/M2 (PKM)	8.42*	3.13*	AEGSDVANAVLDGADCIMLSGETAK, CDENIILWLDYK, NTGIICTIGPASR	AEGSDVANAVLDGADCIMLSGETAK, CDENIILWLDYK, NTGIICTIGPASR
P55859	Purine nucleoside phosphorylase (PNP)	1.25	1.67*	ACVMMQGR	ACVMMQGR
Q2KHU0	Phosphoserine phosphatase (PSPH)	2.49	4.17	FCGVEDAVSEMTR	FCGVEDAVSEMTR
Q58DR8	Succinyl-CoA ligase [GDP-forming] subunit alpha, mitochondrial (SUCLG1)	2.09*	3.18*	IICQGFTGK, LVGPNCPGVINPGECK	IICQGFTGK, LVGPNCPGVINPGECK
P60174	Triosephosphate isomerase (TPI1)	2.01*	3.23*	IAVAAQNCYK, IIYGGSVTGATCK, VPADTEVVCAPPTAYIDFAR	IAVAAQNCYK, IIYGGSVTGATCK, VPADTEVVCAPPTAYIDFAR
Q16831	Uridine phosphorylase 1 (UPP1)	1.21	2.29*	FVCVGGSPSR	FVCVGGSPSR, LDGALCSYTEK
Q99536	Synaptic vesicle membrane protein VAT-1 homolog (VAT1)	2.88*	3.43*	ACGLNFADLMAR	ACGLNFADLMAR, CLVLTGFGGYDK
A7MBG0	Adenylosuccinate synthetase isozyme 2 (ADSS)	N/A	5.08	N/A	MCDLVSDFGGFSER
P13621	ATP synthase subunit O, mitochondrial (ATP5O)	N/A	29	N/A	GEVPCTVTTASALDEATLTELK
Q0IIK5	ATP-dependent RNA helicase DDX1 (DDX1)	N/A	3.78	N/A	GSAFAIGSDGLCCQSR
P68103	Elongation factor 1-alpha 1 (EEF1A1)	N/A	6.23*	N/A	KDGNASGTTLLEALDCILPPTRPTDKPLR, SGDAAIVDMVPGKPMCVESFSDYPPLGR
Q3T094	Protein ETHE1, mitochondrial (ETHE1)	N/A	2.17	N/A	SCTYTYLLGDR
P48035	Fatty acid-binding protein, adipocyte (FABP4)	N/A	2.46*	N/A	MCDAFVGTWK, MVLECVMNGVTATR
P12344	Aspartate aminotransferase, mitochondrial (GOT2)	N/A	4.16	N/A	TCGFDFTGAIEDISK
P19367	Hexokinase-1 (HK1)	N/A	2.2	N/A	CNVSFLLSEDGSGK
P40925	Malate dehydrogenase, cytoplasmic (MDH1)	N/A	2.77	N/A	VIVVGNPANTNCLTASK
Q05B45	Transmembrane protein 120A (TMEM120A)	N/A	1.56	N/A	LQNSCTSSITR
P20000	Aldehyde dehydrogenase, mitochondrial (ALDH2)	2	N/A	LLCGGGAAADR	N/A
Q14195	Dihydropyrimidinase-related protein 3 (DPYSL3)	1.17	N/A	GAPLVVICQGK	N/A
Q71SP7	Fatty acid synthase (FASN)	1.61	N/A	NCLLGMEFSGR	N/A
Protein folding and modification					
P27797	Calreticulin (CALR)	1.41*	2.11*	HEQNIDCGGGYVK	HEQNIDCGGGYVK

TABLE 2. Continued.

ID	Protein name	Ratio to control[a]		SNO-peptides identified[a]	
		VEGF	GSNO	VEGF	GSNO
Q2NKZ1	T-complex protein 1 subunit eta (CCT7)	1.17	5.2	CAMTALSSK, CQVFEETQIGGER	QLCDNAGFDATNILNK
Q3ZCI9	T-complex protein 1 subunit theta (CCT8)	2.84*	4.25	AHEILPDLVC§CSAK, IAVYSCPFDGMITETK	IAVYSCPFDGMITETK
P25417	Cystatin-B (CSTB)	7.03	10.2	MMCGGTSATQPATAETQAIADK	MMCGGTSATQPATAETQAIADK
Q27965	Heat shock 70 kDa protein 1B (HSPA1B)	2.14	2.58*	FEELCSDLFR	ELEQVCNPIISR, FEELCSDLFR
P34932	Heat shock 70 kDa protein 4 (HSPA4)	1.63	2.62*	GCALQCAILSPAFK	GCALQC§AILSPAFK, SVMDATQIAGLNCLR
P11142	Heat shock cognate 71 kDa protein (HSPA8)	1.22	2.2	CNEIINWLDK, VCNPIITK	CNEIINWLDK
P31081	60 kDa heat shock protein, mitochondrial (HSPD1)	3.82*	3.81*	CEFQDAYVLLSEK, CIPALESITPANEDQK	CEFQDAYVLLSEK, CIPALESITPANEDQK, AAVEEGIVLGGGCALLR
Q92743	Serine protease HTRA1 (HTRA1)	2.98	2.67	GACGQGQEDPNSLR	GACGQGQEDPNSLR
P00727	Cytosol aminopeptidase (LAP3)	1.73*	2.66*	AAVAAGCR, ADMGGAATICSAIVSAAK, QVIDCQLADVNNIGK, SAGACTAAAFLK	AAVAAGCR, ADMGGAATICSAIVSAAK, LDLPINIVGLAPLCENMPSGK, QVIDCQLADVNNIGK
Q3T100	Microsomal glutathione S-transferase 3 (MGST3)	2.22*	1.73*	TGLNSGCK, VEYPTMYSTDPENGHIFNCIQR	TGLNSGCK
O43776	Asparaginyl-tRNA synthetase, cytoplasmic (NARS)	1.94*	3.87	LMTDTINEPILLCR	LMTDTINEPILLCR
P30101	Protein disulfide-isomerase A3 (PDIA3)	2.43*	3.43*	FIQENIFGICPHMTEDNKDLIQGK, VDCTANTNTC§NK	VDC§TANTNTC§NK
P62935	Peptidyl-prolyl cis-trans isomerase A (PPIA)	2.53*	5.51*	HTGPGILSMANAGPNTNGSQFFICTAK, IIPGFMCQGGDFTR	HTGPGILSMANAGPNTNGSQFFICTAK, IIPGFMCQGGDFTR
Q15185	Prostaglandin E synthase 3 (PTGES3)	2.12*	2.24	HLNEIDLFHCIDPNDSK, LTFSCLGGSDNFK	LTFSCLGGSDNFK
Q2KJH6	Serpin H1 (SERPINH1)	1.58*	2.10*	QHYNCEHSK	QHYNCEHSK
P17987	T-complex protein 1 subunit alpha (TCP1)	3.11	4.42	GANDFMCDEMER	GANDFMCDEMER
P51176	Protein-glutamine gamma-glutamyl transferase 2 (TGM2)	1.82*	2.97*	DHHTADLCR, SEGTYCCGPVPVR, VVSGMVNCNDDQGVLLGR, TVSYNGILGPECGTK, YCDC§LTESNLIK	DHHTADLCR, SEGTYCCGPVPVR‡, VVSGMVNCNDDQGVLLGR, GCDFDVFAHITNSTPEEHTGR
P09936	Ubiquitin carboxyl-terminal hydrolase isozyme L1 (UCHL1)	2.32*	4.75*	FSAVALCK, NEAIQAAHDAVAQEGQCR	FSAVALCK, NEAIQAAHDAVAQEGQCR
P31800	Cytochrome b-c1 complex subunit 1, mitochondrial (UQCRC1)	1.72	1.94*	LCTSATESEVLR	FTGSQICHR, LCTSATESEVLR
Q3ZBH0	T-complex protein 1 subunit beta (CCT2)	N/A	4.01	N/A	TVYGGGCSEMLMAHAVTQLASR
P49368	T-complex protein 1 subunit gamma (CCT3)	N/A	3.29*	N/A	IPGGIIEDSCVLR, WSSLACNIALDAVK
Q3T0L2	Endoplasmic reticulum resident protein 44 (ERP44)	N/A	5.61	N/A	VDCDQHSDIAQR
P14625	Heat shock protein 90 beta member 1 (HSP90B1)	N/A	6.55	N/A	LTESPCALVASQYGWSGNMER
Q99873	Protein arginine N-methyltransferase 1 (PRMT1)	N/A	3.51*	N/A	GQLCELSC§STDYR, VEDLTFTSPFCLQVK
P25789	Proteasome subunit alpha type-4 (PSMA4)	N/A	10.2	N/A	ATCIGNNSAAAVSMLK
Q32BZ8	Stress-induced-phosphoprotein 1 (STIP1)	N/A	3.51*	N/A	ALDLDSNCK, ALSAGNIDDALQCYSEAIK, AYEDGCK, CVMAQYNR
Q05B50	Ubiquitin-conjugating enzyme E2 D1 (UBE2D1)	N/A	3.17	N/A	IYHPNINSNGSICLDILR
A5PJG7	Cytochrome c-type heme lyase (HCCS)	1.98	N/A	AYEYVQCPITGAK	N/A
Q9UQ80	Proliferation-associated protein 2G4 (PA2G4)	2.32	N/A	AAHLCAEAALR	N/A
P80311	Peptidyl-prolyl cis-trans isomerase B (PPIB)	1.77	N/A	DVTIADCGK	N/A
Cellular signaling and transportation					
P46193	Annexin A1 (ANXA1)	1.93*	3.32*	ILVALCGR, LYGISLCQAILDETKGDYEK, CATSQPMFFAEK	ILVALCGR, LYGISLCQAILDETKGDYEK, LYGISLCQAILDETK
Q9XSA7	Chloride intracellular channel protein 4 (CLIC4)	23.2	13.6*	AGSDGESIGNCPFSQR, DEFTNTCPSDKEVEIAYSDVAK	DEFTNTCPSDK, DEFTNTCPSDKEVEIAYSDVAK
P49951	Clathrin heavy chain1 (CLTC)	1.52*	4.33*	AHIAQLCEK, CNEPAVWSQLAK, HSSLAGCQIINYR	AHIAQLCEK, HSSLAGCQIINYR, IHEGCEEPATHNALAK, VIQCFAETGQVQK
P53621	Coatomer subunit alpha (COPA)	3.73	9.34	CPLSGAC§YSPEFK	CPLSGAC§YSPEFK

TABLE 2. Continued.

ID	Protein name	Ratio to control[a]		SNO-peptides identified[a]	
		VEGF	GSNO	VEGF	GSNO
P50397	Rab GDP dissociation inhibitor beta (GDI2)	1.43*	2.23*	TDDYLDQPCC§ETINR, VICILSHPIK	NTNDANSCQIIPQNQVNR, TDDYLDQPCC§ETINR, VICILSHPIK
P62871	Guanine nucleotide-binding protein G(I)/G(S)/G(T) subunit beta-1 (GNB1)	1.05	2.46*	LFVSGACDASAK	ACADATLSQITNNIDPVGR, ELAGHTGYLSCCR‡, LFVSGACDASAK
Q3T0D0	Heterogeneous nuclear ribonucleoprotein K (HNRNPK)	2.89*	3.33*	LFQEC§CPQSTDR	LFQEC§CPQSTDR
Q5E9A3	Poly(rC)-binding protein 1 (PCBP1)	2.12*	6.12*	AITIAGVPQSVTECVK, INISEGNCPER, LVVPASQCGSLIGK, VMTIPYQPMPASSPVICAGGQDR	INISEGNCPER, VMTIPYQPMPASSPVICAGGQDR
P62998	Ras-related C3 botulinum toxin substrate 1 (RAC1)	1.83*	2.64*	CVVVGDGAVGK, HHCPNTPIILVGTK, YLECSALTQR	CVVVGDGAVGK, HHCPNTPIILVGTK, YLECSALTQR
Q3ZBT1	Transitional endoplasmic reticulum ATPase (VCP)	2.06*	3.00*	VHLGDVISIQPCPDVK	VHLGDVISIQPCPDVK
P45880	Voltage-dependent anion-selective channel protein 2 (VDAC2)	2.53*	3.50*	SCSGVEFSTSGSSNTDTGK, WNTDNTLGTEIAIEDQICQGLK	SCSGVEFSTSGSSNTDTGK, WCEYGLTFTEK
Q2HJG5	Vacuolar protein sorting-associated protein 35 (VPS35)	1.74	2.46	TQCALAASK	TQCALAASK
P09525	Annexin A4 (ANXA4)	N/A	4.4*	N/A	GAGTDEGCLIEILASR
Q9XT28	Copper transport protein ATOX1 (ATOX1)	N/A	5.01	N/A	VCINSEHSVDTLLETLGK
Q2KJ93	Cell division control protein 42 homolog (CDC42)	N/A	2.81*	N/A	CVVVGDGAVGK, YVECSALTQK
Q9NZN4	EH domain-containing protein 2 (EHD2)	N/A	9.26	N/A	IQLEHHISPGDFPDCQK
P11017	Guanine nucleotide-binding protein G(I)/G(S)/G(T) subunit beta-2 (GNB2)	N/A	6.35	N/A	ACGDSTLTQITAGLDPVGR
P63243	Guanine nucleotide-binding protein subunit beta-2-like 1 (GNB2L1)	N/A	2.33*	N/A	FSPNSSNPIIVSCGWDK, YWLCAATGPSIK
P51149	Ras-related protein Rab-7a (RAB7A)	N/A	2.28	N/A	AQAWCYSK
P84095	Rho-related GTP-binding protein RhoG (RHOG)	N/A	3.60*	N/A	CVVVGDGAVGK, YLECSALQQDGVK
Q9NQC3	Reticulon-4 (RTN4)	N/A	2.21	N/A	YSNSALGHVNCTIK
Q05B46	Tricarboxylate transport protein, mitochondrial (SLC25A1)	N/A	1.9	N/A	NTLDCGLQILR
O15198	Mothers against decapentaplegic homolog 9 (SMAD9)	N/A	1.56	N/A	FCLGLLSNVNR
A0JN39	Coatomer subunit beta (COPB1)	1.8	N/A	CIYNLLQSSPAVK	N/A
P08134	Rho-related GTP-binding protein RhoC (RHOC)	1.53*	N/A	HFCPNVPIILVGNKK, LVIVGDGACGK	N/A
A2VDL8	Protein transport protein Sec23A (SEC23A)	1.37	N/A	AVLNPLCQVDYR	N/A
Protein synthese					
O00148	ATP-dependent RNA helicase DDX39 (DDX39A)	1.65*	2.04	NCPHVVVGTPGR	ILYSQCGDVMR
O00571	ATP-dependent RNA helicase DDX3X (DDX3X)	1.61	1.64*	GCHLLVATPGR	DLMACAQTGSGK, GCHLLVATPGR
Q08211	ATP-dependent RNA helicase A (DHX9)	1.47*	2.00*	AAECNIVVTQPR, SSVNCPFSSQDMK	AAECNIVVTQPR, LAAQSCALSLVR, SSVNCPFSSQDMK
P13639	Elongation factor 2 (EEF2)	2.83*	3.88*	CELLYEGPPDDEAAMGIK, CLYASVLTAQPR, EGALCEENMR, KIWCFGPDGTGPNILTDITK, ETVSEESNVLCLSK	CELLYEGPPDDEAAMGIK, CLYASVLTAQPR, EGALCEENMR, KIWCFGPDGTGPNILTDITK, TFCQILLDPIFK
P41091	Eukaryotic translation initiation factor 2 subunit 3 (EIF2S3)	3.28	4.27	IVLTNPVCTEVGEK	IVLTNPVCTEVGEK
P63241	Eukaryotic translation initiation factor 5A-1 (EIF5A)	7.59*	10.10*	KYEDICPSTHNMDVPNIK, MADDLDFETGDAGASATFPMQCSALR, YEDICPSTHNMDVPNIK	KYEDICPSTHNMDVPNIK, MADDLDFETGDAGASATFPMQCSALR
Q96AE4	Far upstream element-binding protein 1 (FUBP1)	1.80*	2.27	IQQESGCK, SCMLTGTPESVQSAK	IQQESGCK

TABLE 2. Continued.

ID	Protein name	Ratio to control[a]		SNO-peptides identified[a]	
		VEGF	GSNO	VEGF	GSNO
P09651	Heterogeneous nuclear ribonucleoprotein A1 (HNRNPA1)	1.12	3.14*	YHTVNGHNCEVR	YHTVNGHNCEVR
A8D8X1	60S ribosomal protein L10 (RPL10)	5.47*	6.60*	MLSCAGADR, VDEFPLCGHMVSDEYEQLSSEALEAAR	VDEFPLCGHMVSDEYEQLSSEALEAAR
P30050	60S ribosomal protein L12 (RPL12)	2.19*	3.01*	CTGGEVGATSALAPK, EILGTAQSVGCNVDGR, HPHDIIDDINSGAVECPAS	CTGGEVGATSALAPK, EILGTAQSVGCNVDGR
Q56JZ1	60S ribosomal protein L13 (RPL13)	2.67	3.06	CTESLQANVQR	CTESLQANVQR
P50914	60S ribosomal protein L14 (RPL14)	1.15	2.05*	ALVDGPCTQVR, CMQLTDFILK	ALVDGPCTQVR, CMQLTDFILK
P62829	60S ribosomal protein L23 (RPL23)	3.05	4.38	ISLGLPVGAVINCADNTGAK	ISLGLPVGAVINCADNTGAK
P46776	60S ribosomal protein L27a (RPL27A)	1.43	2.1	NQSFCPTVNLDK	NQSFCPTVNLDK
P62888	60S ribosomal protein L30 (RPL30)	2.15*	5.14	LVILANNCPALR, VCTLAIIDPGDSDIIR	VCTLAIIDPGDSDIIR
P36578	60S ribosomal protein L4 (RPL4)	2.69*	2.87*	GPCIIYNEDNGIIK, RGPCIIYNEDNGIIK, SGQGAFGNMCR	SGQGAFGNMCR, YAICSALAASALPALVMSK
P62424	60S ribosomal protein L7a (RPL7A)	1.92	3.35	TCTTVAFTQVNSEDK	TCTTVAFTQVNSEDK
P05388	60S acidic ribosomal protein P0 (RPLP0)	1.27	4.49*	CFIVGADNVGSK	AGAIAPCEVTVPAQNTGLGPEK, CFIVGADNVGSK
O18789	40S ribosomal protein S2 (RPS2)	1.15	1.68	GCTATLGNFAK	GCTATLGNFAK
P62857	40S ribosomal protein S28 (RPS28)	0.887	1.26	TGSQGQCTQVR	TGSQGQCTQVR
P61247	40S ribosomal protein S3a (RPS3A)	1.05	1.98*	NCLTNFHGMDLTR	ACQSIYPLHDVFVR, NCLTNFHGMDLTR
P62701	40S ribosomal protein S4, X isoform (RPS4X)	1.36*	2.29*	FDTGNLCMVTGGANLGR	FDTGNLCMVTGGANLGR
A6YRY8	40S ribosomal protein SA (RPSA)	3.53*	4.71*	ADHQPLTEASYVNLPTIALCNTDSPLR	ADHQPLTEASYVNLPTIALCNTDSPLR, YVDIAIPCNNK
P62316	Small nuclear ribonucleoprotein Sm D2 (SNRPD2)	1.11	1.56	HCNMVLENVK	HCNMVLENVK
P17248	Tryptophanyl-tRNA synthetase, cytoplasmic (WARS)	4.58*	5.17*	DRTDVQCLIPC§AIDQDPYFR	DRTDVQCLIPCAIDQDPYFR, GIFGFTDSDCIGK, TDVQCLIPCAIDQDPYFR
Q0II26	Aminoacyl tRNA synthase complex-interacting multifunctional protein 2 (AIMP2)	N/A	4	N/A	QTGGCGGMAPANVQK
P51991	Heterogeneous nuclear ribonucleoprotein A3 (HNRNPA3)	N/A	2.87*	N/A	WGTLTDCVVMR, YHTINGHNCEVK
P31943	Heterogeneous nuclear ribonucleoprotein H (HNRNPH1)	N/A	2.77*	N/A	DLNYCFSGMSDHR, YGDGGSTFQSTTGHCVHMR
P55769	NHP2-like protein 1 (NHP2L1)	N/A	2.27	N/A	LLDLVQQSCNYK
A7YW98	Arginyl-tRNA synthetase, cytoplasmic (RARS)	N/A	1.59	N/A	MDALVAHCSAR
P62906	60S ribosomal protein L10a (RPL10A)	N/A	4.06	N/A	FSVCVLGDQQHC§DEAK
P39023	60S ribosomal protein L3 (RPL3)	N/A	0.97	N/A	VACIGAWHPAR
P62910	60S ribosomal protein L32 (RPL32)	N/A	7.96	N/A	SYCAEIAHNVSSK
P62280	40S ribosomal protein S11 (RPS11)	N/A	2.26*	N/A	CPFTGNVSIR, DVQIGDIVTGECRPLSK, NMSVHLSPCFR
P63220	40S ribosomal protein S21 (RPS21)	N/A	1.85	N/A	TYAICGAIR
P46782	40S ribosomal protein S5 (RPS5)	N/A	2.29*	N/A	KAQCPIVER, VNQAIWLLCTGAR
P40429	60S ribosomal protein L13a (RPL13A)	1.5	N/A	CEGINISGNFYR	N/A
Q07020	60S ribosomal protein L18 (RPL18)	1.24	N/A	GCCGTVLLSGPR	N/A
P49207	60S ribosomal protein L34 (RPL34)	1.1	N/A	AYGGSMCAK	N/A
Q02878	60S ribosomal protein L6 (RPL6)	1.48*	N/A	GKPHCSR	N/A
P62249	40S ribosomal protein S16 (RPS16)	1.38	N/A	TATAVAHCK	N/A
Q07955	Splicing factor, arginine/serine-rich 1 (SFRS1)	2.15*	N/A	EAGDVCYADVVR, GPAGNNDCR	N/A
Other					
P39687	Acidic leucine-rich nuclear phosphoprotein 32 family member A (ANP32A)	1.1	1.94	CPNLTLHLNLSGNK	CPNLTYLNLSGNK
Q6A1I3	Acidic leucine-rich nuclear phosphoprotein 32 family member B (ANP32B)	1.38*	2.05*	ICGGLDMLAEK	ICGGLDMLAEK

13

TABLE 2. *Continued.*

ID	Protein name	Ratio to control[a]		SNO-peptides identified[a]	
		VEGF	GSNO	VEGF	GSNO
P56965	N(G),N(G)-dimethylarginine dimethylaminohydrolase 1 (DDAH1)	6.21	5.48*	LTVPDDTAANCIYLNIPSK	SFCSMAGPNLIAIGSSESAQK
P28801	Glutathione S-transferase P (GSTP1)	1.94	3.09*	ASCIYGQLPK, IHQVLAPSCLDSFPLLSAYVAR	ASCIYGQLPK, IHQVLAPSCLDSFPLLSAYVAR
Q1ZZU7	Macrophage migration inhibitory factor (MIF)	1.16	1.68	LLCGLLTER	LLCGLLTER
Q8MJ50	Osteoclast-stimulating factor 1 (OSTF1)	5.1	5.31	LALDMATNAACASLLK	LALDMATNAACASLLK
P02584	Profilin-1 (PFN1)	1.53*	3.34*	CYEMASHLR, KCYEMASHLR	CYEMASHLR, KCYEMASHLR
P43243	Matrin-3 (MATR3)	N/A	4.35	N/A	LCSLFYTNEEVAK
Q5VZF2	Muscleblind-like protein 2 (MBNL2)	N/A	2.29*	N/A	SCQVENGR
P11940	Polyadenylate-binding protein 1 (PABPC1)	N/A	5.37*	N/A	GFGFVCFSSPEEATK, VVCDENGSK
P0CG38	POTE ankyrin domain family member I (POTEI)	N/A	7.59*	N/A	EKLCYVALDFEQEMAMAASSSLEK
P62714	Serine/threonine-protein phosphatase 2A catalytic subunit beta isoform (PP2CB)	N/A	8.15	N/A	CGNQAAIMELDDTLK
P23193	Transcription elongation factor A protein 1 (TCEA1)	N/A	1.34	N/A	NCTYTQVQTR
P58546	Myotrophin (MTPN)	2.56	N/A	MCDKEFMWALK	N/A
Q3SYU9	Major vault protein (MVP)	1.94	N/A	HYCMVANPVAR	N/A

a N/A, not detected.
* Significant changes ($P < 0.05$ among three independent experiments).
§ The SNO-cysteine in the identified peptides containing two or more cysteines.
‡ The SNO-cysteine was not determined in the identified peptides containing two or more cysteines.

the understanding of SNO, none can meet all the criteria of an ideal method for analyzing global protein SNO, at least including specificity, high-throughput unbiased quantitation and, most important, simultaneous identification of SNO sites.

The proteomics approach developed herein offers not only the specificity (BST labeling) and high throughput (MS/MS) required for large-scale analysis of SNO-proteins in paired proteomes but also unbiased quantitation of the changes in SNO-proteins using SILAC technology. Moreover, this method is capable of simultaneously identifying the specific SNO sites (i.e., reactive SNO-cysteine[s]) in each SNO-protein. These advantages make this method perhaps the most powerful method to date for analyzing global protein SNO in cell culture studies. However, there is a chance that some unique regulatory SNO-proteins might not be able to be identified by this method. For instance, if an SNO-protein is present in only one sample, MS/MS analysis will not give paired spectral readouts of light and heavy SNO-peptides from the paired proteomes using SILAC-based quantitative proteomics technology; then this unique SNO-protein will not be picked up. A potential solution for this limitation can be resolved by using a so-called super-SILAC mix [50, 51] that can be a mixture of many different types of cells labeled with heavy AAs as an internal reference to add a ''pseudo''-readout for the sample that does not have the unique SNO-protein.

In this study, 10 ng/ml VEGF and 1 mM GSNO were chosen to treat endothelial cells for 30 min to prepare the starting materials for comparing the VEGFA- and GSNO-responsive endothelial SNO-proteomes for the following reasons. We have determined the optimal dose of VEGFA to be ~10 ng/ml in stimulating eNOS activation and NO production, ERK1/2 and Akt1 signaling, and in vitro angiogenesis with detailed dose-response and time-course studies in many of our publications (reviewed in Chen and Zheng [52]); 1 mM GSNO has been widely used as a potent exogenous NO donor in cell culture studies [53–55]. More recently, we also have compared the effects of 10 ng/ml VEGF and 1 mM GSNO side by side of SNO of cofilin-1 (CFL1) and found that 10 ng/ml VEGF or 1 mM GSNO stimulated comparable SNO responses in CFL-1 in endothelial cells [31]. With these starting materials and the SILAC-based proteomics technology, we are able to quantitatively distinguish the VEGFA-responsive from the GSNO-responsive SNO-proteins in endothelial cells. We have first shown herein that endogenous NO by VEGFA stimulation and exogenous NO from GSNO dynamically regulate endothelial protein SNO, targeting common and different sets of SNO-proteins, including 125 common SNO-proteins in both VEGFA- and GSNO-treated cells and 27 VEGFA-responsive and 61 GSNO-responsive SNO-proteins. SNO of some unique targets are induced in even opposite changes by VEGFA and GSNO. For instance, the SNO level of actin-related protein 3 (ACTR3) is increased by GSNO but decreased by VEGFA treatment (Table 2). Thus, NO donors and endogenous NO stimulated by VEGFA and potentially other physiological stimuli induce different and even opposite biological responses. Of note, the time courses of endothelial SNO responses to stimulation with VEGFA and an NO donor GSNO are quite different (Fig. 1) [31]. Both maximize at 30 min after stimulation; however, VEGFA-induced SNO response returns to baseline, while the GSNO-induced response persists at 60 min. In this study, the responses were analyzed at only one time point (30 min) to develop/validate the SILAC-based method. However, these time courses suggest that SNO is regulated in a spatiotemporal manner in response to stimulation. Further analysis of the detailed SNO responses to VEGFA and GSNO over time is
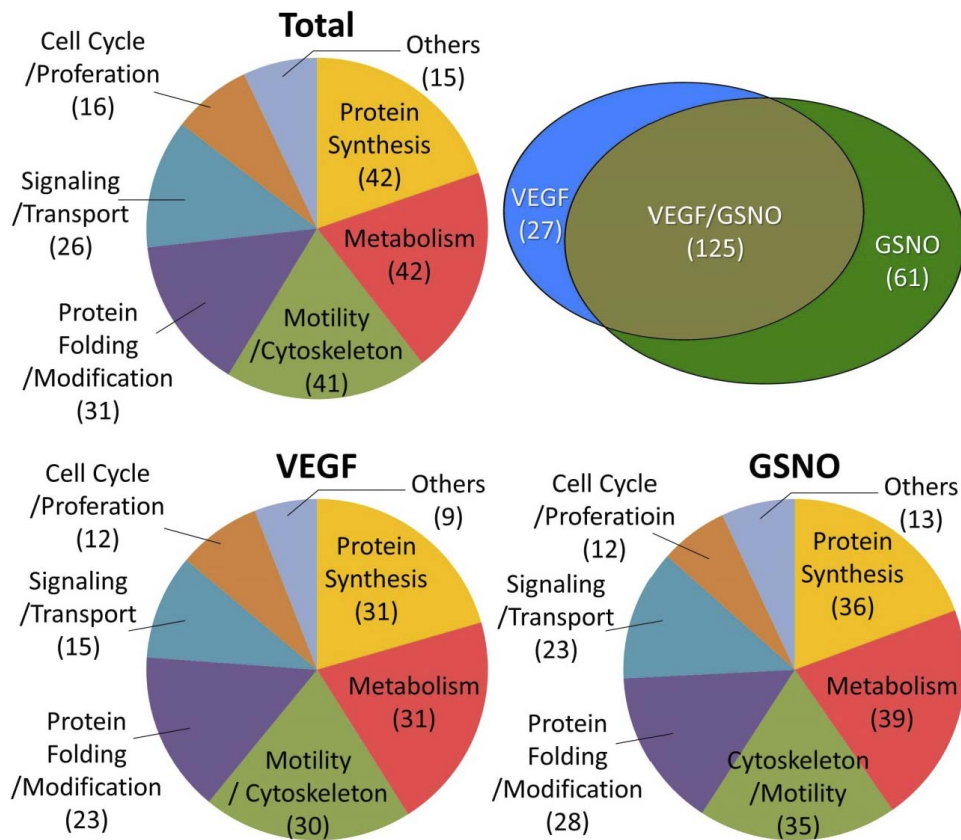
FIG. 6. Summary of the VEGFA- and GSNO-responsive endothelial SNO-proteins. Venn diagram illustrates the overlap of the identified SNO-proteins in oFPAEC treated with VEGFA or GSNO. Pie diagrams illustrate the function classification of the identified SNO-proteins from oFPAEC treated with VEGFA or GSNO, respectively.

needed for revealing important spatiotemporal SNO-protein networks in endothelial cells.

Leading pathway analysis of the 182 VEGFA/GSNO-responsive SNO-proteins (ratio to control >1.3) showed that they are involved in cell cycle and proliferation, cellular cytoskeleton and motility, protein syntheses and modification, cellular signaling and transportation, and metabolism. Of note, we have confirmed herein that CFL1 is one of the VEGFA-responsive SNO target proteins as revealed in our previous studies using different approaches [31]. The primary function of CFL1 is to regulate cytoskeleton remodeling via depolymerizing/severing actin filaments [56]. Our previous work has shown that SNO on CFL1 inhibits the VEGFA-stimulated filopodium formation in endothelial cells [31]. The SNO-dependent mechanism(s) of CFL1 has been demonstrated to regulate VEGFA-induced endothelial cell migration occurring at the early stage of cell migration by affecting filopodium formation, therefore mediating the VEGFA-induced angiogenesis response [31].

In addition to CFL1, a subset of proteins was identified as VEGFA-responsive SNO-proteins whose functions are associated with actin dynamics and cytoskeleton remodeling [57], including myosin, fasin, and actin-related protein 2/3 complex (ARP2/3). Myosin is a member of the ATP-dependent motor proteins responsible for actin-based motility [58]. Myosin-based contraction of filamentous actin (F-actin) is an important determinant of endothelial cell stiffness [59], which is a mechanical property of the vessel wall that affects blood pressure, permeability, and inflammation. It has been recently reported that SNO significantly reduces the Mg^{2+}-ATPase activity of myosin [60], suggesting myosin to be an important

regulatory target for vascular wall health via SNO. Consistent with our previous reports [17, 61], fasin is another VEGFA-responsive SNO-protein that is an actin cross-linking protein present at the leading edges and borders of cells and is well known for its role in promoting cell invasion and migration in vitro [62]. ARP2/3 complex coordinates signals to the actin cytoskeleton and initiates F-actin assembly in response to stimulation [63]. Cyclase-associated protein 1 promotes rapid actin dynamics in conjunction with cofilin [64]. F-actin capping protein caps barbed ends of the actin filament to limit growth of the newly formed actin filament [65]. These findings indicate that SNO is an important mechanism for mediating VEGFA-induced actin dynamics and cytoskeleton remodeling.

There are 12 VEGFA-responsive SNO-proteins that are involved in cell cycle and proliferation, including calpain-2 catalytic subunit, calpain small subunit 1, galectin-1, poly (rC)-binding protein 2, GTP-binding nuclear protein Ran, protein S100-A11, interleukin enhancer-binding factor 3, DNA replication licensing factor MCM5, and four 14-3-3 proteins. The calpains, a ubiquitous family of calcium-dependent cytosolic cysteine proteases, are thought to initiate cytoskeletal breakdown by cleaving proteins important in linking components of the cytoskeleton together and to the cell membrane [66]. NO inhibits cytoskeletal breakdown in skeletal muscle cells by inhibiting calpain cleavage activity via SNO, thereby protecting the cells from ionophore-induced proteolysis [67]. Previous studies have shown that calpain proteolysis may proteolytically disorganize VE-cadherin and subsequently accelerate atherosclerosis [68], suggesting that SNO-mediated calpain activity may provide a therapeutic approach to protect the endothelium from injury or disease. Galectins are members
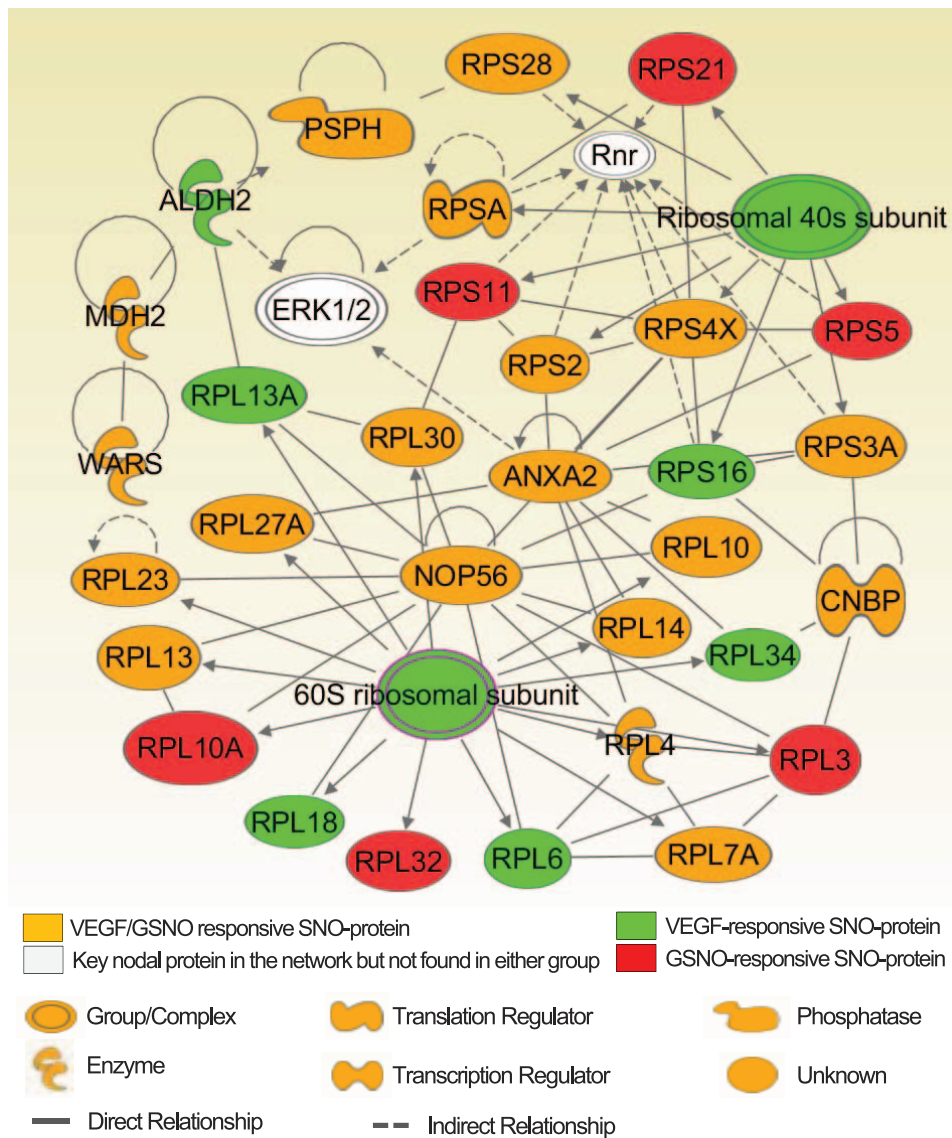
FIG. 7.   VEGFA- and GNSO-induced endothelial SNO-protein networks. Networks of the VEGFA/GSNO-responsive endothelial SNO-proteins were generated by using IPA. Proteins were represented as nodes, and the biological relationship between two nodes is represented as a line. All lines are supported by at least one published reference. Solid lines represent a direct relationship, and dashed lines represent an indirect relationship. The solid and broken semicircles on some proteins indicate direct/indirect self-regulation, i.e., positive or negative feedback, respectively. Lines or semicircles with arrows stand for stimulation or activation on downstream targets. The green (or red) node represents VEGFA (or GSNO) stimulation, respectively, and the yellow node represents stimulation by both VEGFA and GSNO. The shape of each node represents the functional class of proteins.

of a highly conserved family of β-galactoside-binding animal lectins and can differentially affect cellular maturation and function. NO accelerates oxidization of galectin-1 [69], affecting galectin-1 function in promoting proliferation of adult neural stem cells [70]. Galectin also can enhance the survival of breast cancer cells against NO and peroxinitrite during experimental hepatic ischemia-reperfusion injury or direct treatment [71], indicating a potential protective mechanism of SNO on galectin in cell proliferation and against apoptosis. The cellular function of poly (rC)-binding protein 2 is to form ribonucleoprotein complexes with cellular mRNAs, which regulate mRNA stability and translation [72]. GTP-binding nuclear protein Ran, a Ran-GTPase, is involved in nucleocytoplasmic protein import and plays a role in the cell cycle [73]. Ran has been previously identified as an SNO-protein in mouse lung alveolar type II epithelial cells treated with exogenous NO donors [74]. DNA replication licensing factor MCM5 is a member of a family of minichromosome maintenance factors, which is responsible for restricting DNA synthesis only once per cell cycle [75]. The 14-3-3 proteins form a highly conserved family of acidic dimeric proteins with a subunit mass of approximately 30 kDa; overall, they inhibit cell cycle progression and apoptosis and may act as stimulatory or inhibitory factors in signal transduction [76]. Overall these VEGFA-responsive SNO targets are important to mediate the angiogenic effects of VEGFA.

   Among the 125 proteins that are common SNO targets responsive to both VEGFA and GSNO, the SNO response to GSNO is in general greater than that of VEGFA. Interestingly, a cysteine-containing peptide, ILYSQCGDVMR (SNO site underlined), is identified in myosin light polypeptide 6 in both VEGFA- and GSNO-treated cells, whereas another cysteine-containing peptide, MCDFTEDQTAEFK (SNO site underlined), is found only in the VEGFA-treated cells. These results

show that VEGFA and GSNO stimulate SNO of the same protein on different SNO sites. In keeping with our recent functional studies showing that VEGFA and estrogens regulate CFL1 function via SNO on different sites [31, 38], these results not only show the complexity of SNO in regulating protein function but also strengthen the importance of identifying specific SNO sites for delineating the function of SNO in a specific protein in response to different stimulation.

We have successfully developed a BST/SILAC-based quantitative proteomics method for unbiased analysis of global SNO with identification of the specific SNO sites simultaneously. By using this novel assay, we have identified the common and specific SNO protein targets affected by endogenous NO on VEGFA stimulation and exogenous NO from GSNO. Quantitative and leading pathway analysis of the VEGFA- and GSNO-responsive *nitroso*-proteomes reveals that SNO is a critical mechanism for VEGFA stimulation of endothelial cell proliferation and motility, which are critical steps for angiogenesis. With the identification of specific SNO sites in each SNO-protein, the VEGFA- and GSNO-responsive endothelial *nitroso*-proteomes identified herein provide fundamental databases for delineating the functional significance of SNO in endothelial cell biology.

REFERENCES

1. Beckman JS, Koppenol WH. Nitric oxide, superoxide, and peroxynitrite: the good, the bad, and ugly. Am J Physiol 1996; 271:C1424–C1437.
2. Lamalice L, Le Boeuf F, Huot J. Endothelial cell migration during angiogenesis. Circ Res 2007; 100:782–794.
3. Morbidelli L, Chang CH, Douglas JG, Granger HJ, Ledda F, Ziche M. Nitric oxide mediates mitogenic effect of VEGF on coronary venular endothelium. Am J Physiol 1996; 270:H411–H415.
4. Papapetropoulos A, Garcia-Cardena G, Madri JA, Sessa WC. Nitric oxide production contributes to the angiogenic properties of vascular endothelial growth factor in human endothelial cells. J Clin Invest 1997; 100: 3131–3139.
5. Arnold WP, Mittal CK, Katsuki S, Murad F. Nitric oxide activates guanylate cyclase and increases guanosine 3′:5′-cyclic monophosphate levels in various tissue preparations. Proc Natl Acad Sci U S A 1977; 74: 3203–3207.
6. Hess DT, Matsumoto A, Kim SO, Marshall HE, Stamler JS. Protein *S*-nitrosylation: purview and parameters. Nat Rev Mol Cell Biol 2005; 6: 150–166.
7. Lane P, Hao G, Gross SS. *S*-nitrosylation is emerging as a specific and fundamental posttranslational protein modification: head-to-head comparison with O-phosphorylation. Sci STKE 2001; 2001:RE1.
8. Bartlett GJ, Porter CT, Borkakoti N, Thornton JM. Analysis of catalytic residues in enzyme active sites. J Mol Biol 2002; 324:105–121.
9. Hess DT, Matsumoto A, Nudelman R, Stamler JS. *S*-nitrosylation: spectrum and specificity. Nat Cell Biol 2001; 3:E46–E49.
10. Stamler JS, Lamas S, Fang FC. Nitrosylation: the prototypic redox-based signaling mechanism. Cell 2001; 106:675–683.
11. Anand P, Stamler JS. Enzymatic mechanisms regulating protein *S*-nitrosylation: implications in health and disease. J Mol Med (Berl) 2012; 90:233–244.
12. Lima B, Forrester MT, Hess DT, Stamler JS. *S*-nitrosylation in cardiovascular signaling. Circ Res 2010; 106:633–646.
13. Liu L, Yan Y, Zeng M, Zhang J, Hanes MA, Ahearn G, McMahon TJ, Dickfeld T, Marshall HE, Que LG, Stamler JS. Essential roles of S-nitrosothiols in vascular homeostasis and endotoxic shock. Cell 2004; 116: 617–628.
14. Zhang HH, Wang YP, Chen DB. Analysis of nitroso-proteomes in normotensive and severe preeclamptic human placentas. Biol Reprod 2011; 84:966–975.
15. Jaffrey SR, Snyder SH. The biotin switch method for the detection of S-nitrosylated proteins. Sci STKE 2001; 2001:PL1.
16. Zhang HH, Feng L, Livnat I, Hoh JK, Shim JY, Liao WX, Chen DB. Estradiol-17β stimulates specific receptor and endogenous nitric oxide-dependent dynamic endothelial protein *S*-nitrosylation: analysis of endothelial nitrosyl-proteome. Endocrinology 2010; 151:3874–3887.
17. Zhang HH, Feng L, Wang W, Magness RR, Chen DB. Estrogen-responsive nitroso-proteome in uterine artery endothelial cells: role of

18. endothelial nitric oxide synthase and estrogen receptor-beta. J Cell Physiol 2012; 227:146–159.
18. Aebersold R, Mann M. Mass spectrometry-based proteomics. Nature 2003; 422:198–207.
19. Mann M. Functional and quantitative proteomics using SILAC. Nat Rev Mol Cell Biol 2006; 7:952–958.
20. Ong SE, Blagoev B, Kratchmarova I, Kristensen DB, Steen H, Pandey A, Mann M. Stable isotope labeling by amino acids in cell culture, SILAC, as a simple and accurate approach to expression proteomics. Mol Cell Proteomics 2002; 1:376–386.
21. Liao WX, Feng L, Zhang H, Zheng J, Moore TR, Chen DB. Compartmentalizing VEGF-induced ERK2/1 signaling in placental artery endothelial cell caveolae: a paradoxical role of caveolin-1 in placental angiogenesis in vitro. Mol Endocrinol 2009; 23:1428–1444.
22. Mata-Greenwood E, Jenkins C, Farrow KN, Konduri GG, Russell JA, Lakshminrusimha S, Black SM, Steinhorn RH. eNOS function is developmentally regulated: uncoupling of eNOS occurs postnatally. Am J Physiol Lung Cell Mol Physiol 2006; 290:L232–L241.
23. Acker SN, Seedorf GJ, Abman SH, Nozik-Grayck E, Partrick DA, Gien J. Pulmonary artery endothelial cell dysfunction and decreased populations of highly proliferative endothelial cells in experimental congenital diaphragmatic hernia. Am J Physiol Lung Cell Mol Physiol 2013; 305: L943–L952.
24. Heller R, Polack T, Grabner R, Till U. Nitric oxide inhibits proliferation of human endothelial cells via a mechanism independent of cGMP. Atherosclerosis 1999; 144:49–57.
25. Thibeault S, Rautureau Y, Oubaha M, Faubert D, Wilkes BC, Delisle C, Gratton JP. *S*-nitrosylation of beta-catenin by eNOS-derived NO promotes VEGF-induced endothelial cell permeability. Mol Cell 2010; 39:468–476.
26. Camejo D, Romero-Puertas Mdel C, Rodriguez-Serrano M, Sandalio LM, Lazaro JJ, Jimenez A, Sevilla F. Salinity-induced changes in *S*-nitrosylation of pea mitochondrial proteins. J Proteomics 2013; 79:87–99.
27. Chen DB, Bird IM, Zheng J, Magness RR. Membrane estrogen receptor-dependent extracellular signal-regulated kinase pathway mediates acute activation of endothelial nitric oxide synthase by estrogen in uterine artery endothelial cells. Endocrinology 2004; 145:113–125.
28. Fang L, Wang X, Yamoah K, Chen PL, Pan ZQ, Huang L. Characterization of the human COP9 signalosome complex using affinity purification and mass spectrometry. J Proteome Res 2008; 7:4914–4925.
29. Satohisa S, Zhang HH, Feng L, Yang YY, Huang L, Chen DB. Endogenous NO upon estradiol-17β stimulation and NO donor differentially regulate mitochondrial *S*-nitrosylation in endothelial cells. Endocrinology 2014; 155:3005–3016.
30. Guerrero C, Tagwerker C, Kaiser P, Huang L. An integrated mass spectrometry-based proteomic approach: quantitative analysis of tandem affinity-purified in vivo cross-linked protein complexes (QTAX) to decipher the 26 S proteasome-interacting network. Mol Cell Proteomics 2006; 5:366–378.
31. Zhang HH, Wang W, Feng L, Yang Y, Zheng J, Huang L, Chen DB. *S*-nitrosylation of Cofilin-1 serves as a novel pathway for VEGF-stimulated endothelial cell migration. J Cell Physiol 2015; 230:406–417.
32. Dhungana S, Merrick BA, Tomer KB, Fessler MB. Quantitative proteomics analysis of macrophage rafts reveals compartmentalized activation of the proteasome and of proteasome-mediated ERK activation in response to lipopolysaccharide. Mol Cell Proteomics 2009; 8:201–213.
33. Zhou X, Han P, Li J, Zhang X, Huang B, Ruan HQ, Chen C. ESNOQ, proteomic quantification of endogenous S-nitrosation. PLoS One 2010; 5: e10015.
34. Lin MI, Fulton D, Babbitt R, Fleming I, Busse R, Pritchard KA Jr, Sessa WC. Phosphorylation of threonine 497 in endothelial nitric-oxide synthase coordinates the coupling of L-arginine metabolism to efficient nitric oxide production. J Biol Chem 2003; 278:44719–44726.
35. Zheng J, Wen Y, Austin JL, Chen DB. Exogenous nitric oxide stimulates cell proliferation via activation of a mitogen-activated protein kinase pathway in ovine fetoplacental artery endothelial cells. Biol Reprod 2006; 74:375–382.
36. Whitley E, Ball J. Statistics review 4: sample size calculations. Crit Care 2002; 6:335–341.
37. McCarthy DJ, Smyth GK. Testing significance relative to a fold-change threshold is a TREAT. Bioinformatics 2009; 25:765–771.
38. Zhang HH, Lechuga TJ, Tith T, Wang W, Wing DA, Chen DB. *S*-nitrosylation of cofilin-1 mediates estradiol-17β-stimulated endothelial cytoskeleton remodeling. Mol Endocrinol 2015; 29:434–444.
39. Liao WX, Feng L, Zheng J, Chen DB. Deciphering mechanisms controlling placental artery endothelial cell migration stimulated by vascular endothelial growth factor. Endocrinology 2009; 151:3432–3444.
40. Zheng J, Bird IM, Melsaether AN, Magness RR. Activation of the

mitogen-activated protein kinase cascade is necessary but not sufficient for basic fibroblast growth factor- and epidermal growth factor-stimulated expression of endothelial nitric oxide synthase in ovine fetoplacental artery endothelial cells. Endocrinology 1999; 140:1399–1407.

41. Cooke JP. NO and angiogenesis. Atheroscler Suppl 2003; 4:53–60.

42. Searles CD. Transcriptional and posttranscriptional regulation of endothelial nitric oxide synthase expression. Am J Physiol Cell Physiol 2006; 291:C803–C816.

43. Smith JN, Dasgupta TP. Kinetics and mechanism of the decomposition of S-nitrosoglutathione by l-ascorbic acid and copper ions in aqueous solution to produce nitric oxide. Nitric Oxide 2000; 4:57–66.

44. Dicks AP, Williams DL. Generation of nitric oxide from S-nitrosothiols using protein-bound Cu2+ sources. Chem Biol 1996; 3:655–659.

45. Torta F, Usuelli V, Malgaroli A, Bachi A. Proteomic analysis of protein S-nitrosylation. Proteomics 2008; 8:4484–4494.

46. Yang Y, Loscalzo J. S-nitrosoprotein formation and localization in endothelial cells. Proc Natl Acad Sci U S A 2005; 102:117–122.

47. Forrester MT, Thompson JW, Foster MW, Nogueira L, Moseley MA, Stamler JS. Proteomic analysis of S-nitrosylation and denitrosylation by resin-assisted capture. Nat Biotechnol 2009; 27:557–559.

48. Hao G, Derakhshan B, Shi L, Campagne F, Gross SS. SNOSID, a proteomic method for identification of cysteine S-nitrosylation sites in complex protein mixtures. Proc Natl Acad Sci U S A 2006; 103: 1012–1017.

49. Camerini S, Polci ML, Restuccia U, Usuelli V, Malgaroli A, Bachi A. A novel approach to identify proteins modified by nitric oxide: the HIS-TAG switch method. J Proteome Res 2007; 6:3224–3231.

50. Aasebo E, Vaudel M, Mjaavatten O, Gausdal G, Van der Burgh A, Gjertsen BT, Doskeland SO, Bruserud O, Berven FS, Selheim F. Performance of super-SILAC based quantitative proteomics for comparison of different acute myeloid leukemia (AML) cell lines. Proteomics 14: 1971–1976.

51. Geiger T, Cox J, Ostasiewicz P, Wisniewski JR, Mann M. Super-SILAC mix for quantitative proteomics of human tumor tissue. Nat Methods 2010; 7:383–385.

52. Chen DB, Zheng J. Regulation of placental angiogenesis. Microcirculation 2014; 21:15–25.

53. Metzen E, Zhou J, Jelkmann W, Fandrey J, Brune B. Nitric oxide impairs normoxic degradation of HIF-1alpha by inhibition of prolyl hydroxylases. Mol Biol Cell 2003; 14:3470–3481.

54. Wang P, Liu GH, Wu K, Qu J, Huang B, Zhang X, Zhou X, Gerace L, Chen C. Repression of classical nuclear export by S-nitrosylation of CRM1. J Cell Sci 2009; 122:3772–3779.

55. Zaffagnini M, Morisse S, Bedhomme M, Marchand CH, Festa M, Rouhier N, Lemaire SD, Trost P. Mechanisms of nitrosylation and denitrosylation of cytoplasmic glyceraldehyde-3-phosphate dehydrogenase from Arabidopsis thaliana. J Biol Chem 2013; 288:22777–22789.

56. Theriot JA. Accelerating on a treadmill: ADF/cofilin promotes rapid actin filament turnover in the dynamic cytoskeleton. J Cell Biol 1997; 136: 1165–1168.

57. Janmey PA. The cytoskeleton and cell signaling: component localization and mechanical coupling. Physiol Rev 1998; 78:763–781.

58. Mitchison TJ, Cramer LP. Actin-based cell motility and cell locomotion. Cell 1996; 84:371–379.

59. Huveneers S, Daemen MJ, Hordijk PL. Between Rho(k) and a hard place: the relation between vessel wall stiffness, endothelial contractility, and cardiovascular disease. Circ Res 2015; 116:895–908.

60. Nogueira L, Figueiredo-Freitas C, Casimiro-Lopes G, Magdesian MH, Assreuy J, Sorenson MM. Myosin is reversibly inhibited by S-nitrosylation. Biochem J 2009; 424:221–231.

61. Wu C, Parrott AM, Liu T, Jain MR, Yang Y, Sadoshima J, Li H. Distinction of thioredoxin transnitrosylation and denitrosylation target proteins by the ICAT quantitative approach. J Proteomics 2011; 74: 2498–2509.

62. Hashimoto Y, Kim DJ, Adams JC. The roles of fascins in health and disease. J Pathol 2011; 224:289–300.

63. Machesky LM, Gould KL. The Arp2/3 complex: a multifunctional actin organizer. Curr Opin Cell Biol 1999; 11:117–121.

64. Bertling E, Hotulainen P, Mattila PK, Matilainen T, Salminen M, Lappalainen P. Cyclase-associated protein 1 (CAP1) promotes cofilin-induced actin dynamics in mammalian nonmuscle cells. Mol Biol Cell 2004; 15:2324–2334.

65. McGregor E, Kempster L, Wait R, Gosling M, Dunn MJ, Powell JT. F-actin capping (CapZ) and other contractile saphenous vein smooth muscle proteins are altered by hemodynamic stress: a proteonomic approach. Mol Cell Proteomics 2004; 3:115–124.

66. Huang J, Forsberg NE. Role of calpain in skeletal-muscle protein degradation. Proc Natl Acad Sci U S A 1998; 95:12100–12105.

67. Koh TJ, Tidball JG. Nitric oxide inhibits calpain-mediated proteolysis of talin in skeletal muscle cells. Am J Physiol Cell Physiol 2000; 279: C806–C812.

68. Miyazaki T, Taketomi Y, Takimoto M, Lei XF, Arita S, Kim-Kaneyama JR, Arata S, Ohata H, Ota H, Murakami M, Miyazaki A. m-Calpain induction in vascular endothelial cells on human and mouse atheromas and its roles in VE-cadherin disorganization and atherosclerosis. Circulation 2011; 124:2522–2532.

69. Levy D, Tal M, Hoke A, Zochodne DW. Transient action of the endothelial constitutive nitric oxide synthase (ecNOS) mediates the development of thermal hypersensitivity following peripheral nerve injury. Eur J Neurosci 2000; 12:2323–2332.

70. Sakaguchi M, Shingo T, Shimazaki T, Okano HJ, Shiwa M, Ishibashi S, Oguro H, Ninomiya M, Kadoya T, Horie H, Shibuya A, Mizusawa H, et al. A carbohydrate-binding protein, Galectin-1, promotes proliferation of adult neural stem cells. Proc Natl Acad Sci U S A 2006; 103:7112–7117.

71. Song YK, Billiar TR, Lee YJ. Role of galectin-3 in breast cancer metastasis: involvement of nitric oxide. Am J Pathol 2002; 160: 1069–1075.

72. Holcik M, Liebhaber SA. Four highly stable eukaryotic mRNAs assemble 3′ untranslated region RNA-protein complexes sharing cis and trans components. Proc Natl Acad Sci U S A 1997; 94:2410–2414.

73. Hughes M, Zhang C, Avis JM, Hutchison CJ, Clarke PR. The role of the ran GTPase in nuclear assembly and DNA replication: characterisation of the effects of Ran mutants. J Cell Sci 1998; 111(pt 20):3017–3026.

74. Ckless K, Reynaert NL, Taatjes DJ, Lounsbury KM, van der Vliet A, Janssen-Heininger Y. In situ detection and visualization of S-nitrosylated proteins following chemical derivatization: identification of Ran GTPase as a target for S-nitrosylation. Nitric Oxide 2004; 11:216–227.

75. Tye BK. MCM proteins in DNA replication. Annu Rev Biochem 1999; 68:649–686.

76. van Hemert MJ, Steensma HY, van Heusden GP. 14-3-3 proteins: key regulators of cell division, signalling and apoptosis. Bioessays 2001; 23: 936–946.